Neuronal FcγRI mediates acute and chronic joint pain

Li Wang,[1] Xiaohua Jiang,[1] Qin Zheng,[2] Sang-Min Jeon,[1] Tiane Chen,[1] Yan Liu,[1] Heather Kulaga,[3] Randall Reed,[3] Xinzhong Dong,[2] Michael J. Caterina,[1,2,4] and Lintao Qu[1]

[1]Department of Neurosurgery and Neurosurgery Pain Research Institute, [2]Solomon H. Snyder Department of Neuroscience, [3]Department of Molecular Biology and Genetics, and [4]Department of Biological Chemistry, Johns Hopkins University School of Medicine, Baltimore, Maryland, USA.

Although joint pain in rheumatoid arthritis (RA) is conventionally thought to result from inflammation, arthritis pain and joint inflammation are at least partially uncoupled. This suggests that additional pain mechanisms in RA remain to be explored. Here we show that FcγRI, an immune receptor for IgG immune complex (IgG-IC), is expressed in a subpopulation of joint sensory neurons and that, under naive conditions, FcγRI cross-linking by IgG-IC directly activates the somata and peripheral terminals of these neurons to evoke acute joint hypernociception without obvious concurrent joint inflammation. These effects were diminished in both global and sensory neuron–specific *Fcgr1*-knockout mice. In murine models of inflammatory arthritis, FcγRI signaling was upregulated in joint sensory neurons. Acute blockade or global genetic deletion of *Fcgr1* significantly attenuated arthritis pain and hyperactivity of joint sensory neurons without measurably altering joint inflammation. Conditional deletion of *Fcgr1* in sensory neurons produced similar analgesic effects in these models. We therefore suggest that FcγRI expressed in sensory neurons contributes to arthritis pain independently of its functions in inflammatory cells. These findings expand our understanding of the immunosensory capabilities of sensory neurons and imply that neuronal FcγRI merits consideration as a target for treating RA pain.

Introduction

Rheumatoid arthritis (RA) is a chronic autoimmune disorder that affects millions of American adults and exhibits high morbidity and mortality. Joint pain is a cardinal clinical feature of RA, and poses an enormous health burden (1, 2). RA is characterized by synovitis and joint destruction, both of which are significant contributors to the associated joint pain. Accordingly, most current treatments for RA pain are aimed at reducing joint inflammation and slowing joint damage. Yet many of these antiinflammatory therapies exhibit limited efficacy and/or adverse side effects (3, 4). While RA pain is often viewed simply as a direct consequence of inflammation, pain and inflammation are at least partially uncoupled in RA (5, 6). Joint pain often precedes overt signs of joint inflammation and can persist in subpopulations of RA patients despite seemingly optimal control of inflammation with current biologic therapies (7–9). A recent study demonstrated that anti–citrullinated protein antibodies may trigger RA pain via an inflammatory cell–independent mechanism that involves release of the nociceptive chemokine CXCL1/IL-8 from osteoclasts (10). Thus, additional mechanisms besides inflammation likely contribute to RA pain. Yet such mechanisms remain largely unexplored.

One important pathological entity in RA is immunoglobulin G immune complex (IgG-IC), which is present at high amounts in the serum and affected joints of RA patients (11, 12). IgG-IC exerts its biological effects largely through Fcγ receptors (FcγRs), which are most prominently expressed in immune cells and are critical regulators of immunity (13–16). Of 4 FcγR subtypes (I–IV) in rodents, most are low-affinity receptors and only bind IgG in immune complexes. However, FcγRI (also called CD64) is the sole high-affinity receptor that can bind both monomeric and polymeric IgG (16). IgG-IC/FcγRI signaling has been implicated in the pathogenesis of RA. *Fcgr1*-deficient mice exhibited decreased arthritic symptoms in collagen-induced arthritis (CIA) and antigen-induced arthritis (AIA) models (11, 17, 18), and treatment with a CD64-directed immunotoxin diminished inflammation and bone erosion in human CD64–transgenic rats suffering from joint inflammation (19). Similarly, scavenging IgG-IC with recombinant soluble FcγRI suppressed cartilage destruction in AIA and CIA models (11, 20). However, FcγRI plays differential roles in arthritis pathogenesis in different animal models of RA. Whereas FcγRI is of crucial importance in both severe joint inflammation and cartilage destruction in the CIA model (11, 20), in the AIA model this receptor predominantly mediates cartilage destruction without a clear role in joint inflammation (17, 18). Thus, the AIA model enables us to focus on the potential roles of FcγRI in AIA-associated pain beyond those in inflammation, per se.

Although IgG-IC/FcγRI signaling has been suggested to play a prominent role in arthritis pathogenesis (11, 17, 18, 21), there are no reports specifically addressing its potential contributions to RA pain. Given that FcγRI is widely expressed in immune cells (13–16), FcγRI has been thought to contribute to RA pain by inducing proinflammatory cytokine release from immune cells. While multiple cytokines appear to sensitize joint nociceptors (22–26), this cannot explain all components of RA pain. Our group and others have revealed that, in addition to its expression in immune cells, FcγRI, but not subtypes II or III, is also expressed in subsets

Conflict of interest: The authors have declared that no conflict of interest exists.

Submitted: February 8, 2019; **Accepted:** June 11, 2019; **Published:** August 12, 2019.
Reference information: *J Clin Invest*. 2019;129(9):3754–3769.
https://doi.org/10.1172/JCI128010.

of nociceptive dorsal root ganglion (DRG) neurons of rats and mice (27, 28). These neuronal receptors are functional, since in DRG neuron culture, IgG-IC directly induces neuronal activation through a process that involves FcγRI and a downstream ion channel, TRPC3 (29). Yet the in vivo relevance of these findings has not been explored, and no studies have addressed whether FcγRI is expressed in joint sensory neurons or whether IgG-IC acts directly on joint sensory afferents through neuronal FcγRI to induce joint pain. It is also unknown whether neuronal FcγRI contributes to joint hypernociception in the setting of arthritis. In this study, we tested the hypothesis that IgG-IC signaling contributes to RA joint pain, at least in part, through a mechanism involving direct activation of neuronal FcγRI.

Results

FcγRI is expressed in mouse joint-innervating DRG neurons. Since all commercially available anti-FcγRI antibodies that we tested lacked adequate specificity for reliable immunostaining of mouse tissues, we alternatively performed in situ hybridization (ISH) to map the expression pattern of FcγRI in joint-innervating DRG neurons that were retrogradely labeled by fast blue (FB) injection into the ankle joint. ISH revealed *Fcgr1* mRNA expression in 27.5% of FB-labeled joint sensory neurons, regardless of cell size (Figure 1A). *Fcgr1* ISH signal was colocalized with immunostaining for the neuronal-specific nuclear protein NeuN (Figure 1A), suggesting neuronal expression of *Fcgr1* mRNA. The specificity of *Fcgr1* mRNA detection was validated by a loss of ISH signal in the DRG of global *Fcgr1*$^{-/-}$ mice (Figure 1B) and in WT DRG sections stained with a sense control probe (Figure 1C). To further define the expression pattern of FcγRI in joint sensory DRG neurons, we performed double staining for FcγRI and markers of different cell populations. Among FB-labeled joint sensory neurons, *Fcgr1* mRNA expression was detected in both small-diameter (peripherin^{+}) and large-diameter (NF200^{+}) neurons (Figure 1D). In addition, 53.3% of *Fcgr1*$^{+}$ neurons coexpressed CGRP, a marker for nociceptive peptidergic neurons (Figure 1D). However, we did not detect obvious colocalization of *Fcgr1* mRNA expression with glutamine synthetase, a satellite glial cell marker (Figure 1D). These results indicate that a subpopulation of joint sensory neurons, including nociceptors, express FcγRI, providing an anatomical basis for neuronal FcγRI modulation of joint pain.

IgG-IC directly activates joint sensory afferents through neuronal FcγRI. To examine whether the FcγRI expressed in joint sensory neurons is functional, we investigated the effects of IgG-IC on Ca^{2+} responses in dissociated DiI-labeled DRG neurons from WT (*Fcgr1*$^{+/+}$) and global *Fcgr1*$^{-/-}$ mice using ratiometric Ca^{2+} imaging. In *Fcgr1*$^{+/+}$ mice, application of IgG-IC (1 μg/mL), but not antigen (BSA) or antibody alone (anti-BSA IgG), evoked Ca^{2+} increases in 17.6% of joint sensory neurons (Figure 2, A and B). Moreover, 80% of IgG-IC–responsive neurons responded to capsaicin. In contrast, IgG-IC evoked Ca^{2+} responses in a significantly smaller fraction (3.8%) of joint sensory neurons from global *Fcgr1*$^{-/-}$ mice (Figure 2, A and B).

To visualize whether IgG-IC directly activates peripheral terminals of joint sensory afferents through FcγRI, we performed in vivo imaging on the cell bodies of retrogradely DiI-labeled DRG neurons of mice (*PirtCre-GCamp6*), which express the fluorescent calcium indicator GCAMP6 in peripheral sensory neurons (30). Injection of IgG-IC (100 μg/mL; 10 μL), but not vehicle (PBS) or monomeric IgG, to the right hind ankle joint cavity evoked Ca^{2+} responses in a subset of DiI-labeling joint sensory neurons (Figure 2, C and D). Moreover, all IgG-IC–responsive neurons responded to mechanical stimulation when the ankle was pressed with blunt forceps (Figure 2C). However, the proportion of IgG-IC–responsive neurons was significantly diminished in *PirtCre-GCamp6* mice crossed onto global *Fcgr1*$^{-/-}$ mice (Figure 2, C and D). These findings support the idea that IgG-IC has a direct excitatory action on joint sensory afferents via the activation of neuronally expressed FcγRI.

Local administration of IgG-IC elicits acute joint pain–related hypersensitivity without obvious inflammation in naive mice. Given that IgG-IC is able to stimulate immune cells, directly activate joint sensory neurons, or both, we assessed the effects of IgG-IC at different doses on joint pain and inflammatory processes in vivo. Intra-articular (i.a.) injection of IgG-IC, but not the vehicle (PBS) or monomeric IgG, into the right hind ankle cavity of the mouse significantly reduced mechanical response threshold in the hind ankle, and increased hind paw withdrawal frequency to mechanical stimulation of nearby glabrous paw skin in a dose-dependent manner (Figure 3, A–C). No secondary heat hyperalgesia in the hind paw skin or obvious joint swelling was observed after i.a. injection of IgG-IC (Figure 3, D and E). The pronociceptive effects lasted for at least 5 hours after injection and were resolved 24 hours later. Since IgG-IC–evoked nociceptive behaviors may result from joint inflammation, we performed quantitative reverse transcription PCR (RT-qPCR) to assay for changes in a subset of inflammatory markers in the synovium at the early (1 hour) and late (5 hours) phases following i.a. injection of IgG-IC. However, no significant differences were observed in the mRNA expression levels of cytokines (*Tnfa*, *Il6*, *Il1b*), chemokines (*Mcp1*, *Cxcl1*), matrix metalloproteinases (*Mmp2*, *Mmp9*, *Mmp13*), T cell (*Cd3*) or macrophage (*Cd68*) markers, or mast cell proteases (*Mcpt4*, *Tpsb2*) in the joint synovium between treatments at 1 hour (Supplemental Figure 1A; supplemental material available online with this article; https://doi.org/10.1172/JCI128010DS1) and 5 hours (Supplemental Figure 2A) after injection. To further determine whether i.a. injection of IgG-IC induced a local immune response, we used immunohistochemical (IHC) staining to assess cellular infiltration of macrophages, neutrophils, lymphocytes, and mast cells in the joint synovium, using the markers CD68, Ly6G/C, CD3, and c-Kit, respectively. No obvious differences were observed in any of these markers between groups 1 hour after the injection (Figure 3, F and G). However, the expression of Ly6G/C and CD3 in the synovium was significantly increased at 5 hours after injection in IgG-IC–treated mice, compared with those treated with vehicle or monomeric IgG (Supplemental Figure 2, B and C). Likewise, joint histological H&E staining analysis did not reveal any signs of immune cell infiltration or synovial hyperplasia in any groups at 1 hour (Figure 3H) or 5 hours (Supplemental Figure 2D) after injection. In addition, toluidine blue (TB)/fast green staining showed that IgG-IC did not cause any obvious bone or cartilage destruction in the joint compared with controls (Supplemental Figure 1B and Supplemental Figure 2E). These data suggest that IgG-IC is sufficient to evoke behavioral signs of acute joint pain without concurrent inflammation, at least at early stages.

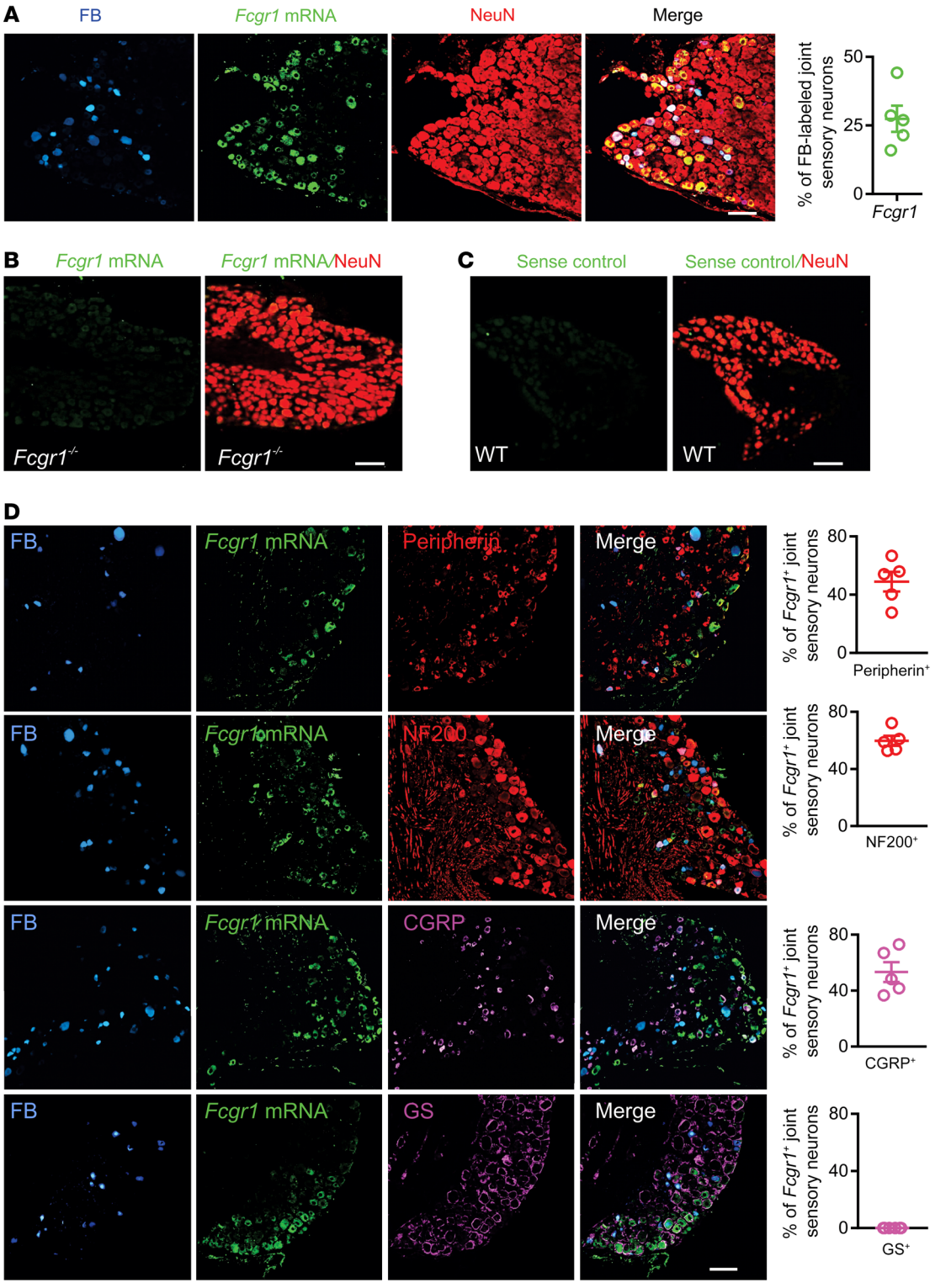

Figure 1. Analysis of FcγRI expression in mouse joint sensory neurons. Joint-innervating DRG neurons were labeled retrogradely by injection of fast blue (FB; 8 μL; 1% in saline) into the ankle cavity at least 2 weeks before harvesting. (**A**) ISH images showing *Fcgr1* mRNA expression (green) in a subset of FB-labeled joint sensory neurons (blue) of WT mice (n = 5 mice). *Fcgr1* signal was colocalized with the pan-neuronal marker NeuN (red). (**B**) ISH image showing absence of *Fcgr1* mRNA expression in DRG neurons of global *Fcgr1*$^{-/-}$ mice (n = 3 mice). (**C**) ISH image of sense control probe (n = 3 mice). (**D**) Fluorescent ISH for *Fcgr1* and immunostaining using antibodies against peripherin (n = 5 mice), NF200 (n = 5 mice), CGRP (n = 5 mice), and glutamine synthetase (GS; n = 6 mice), along with quantitative analysis of percentage overlap. Scale bars: 50 μm.

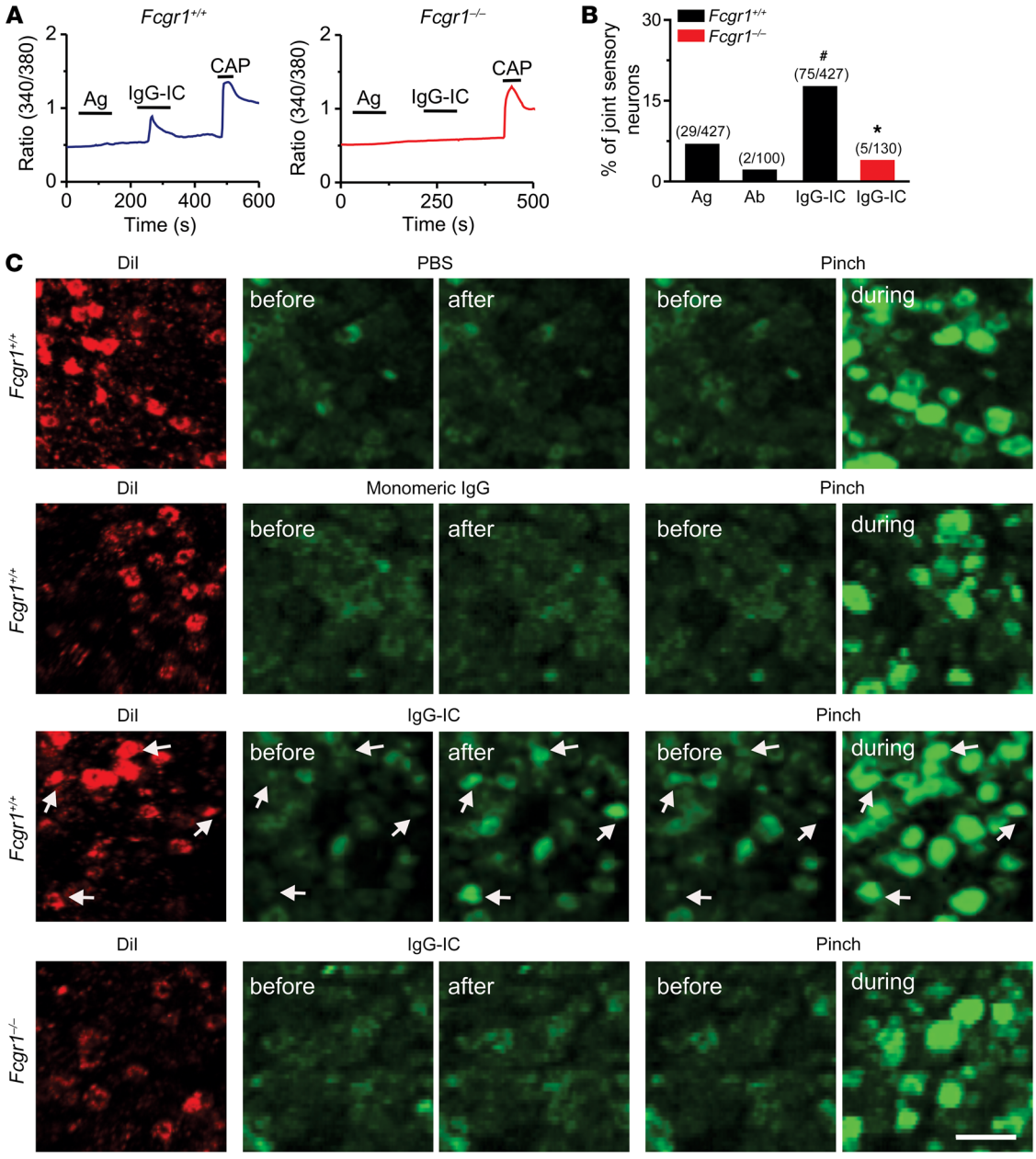

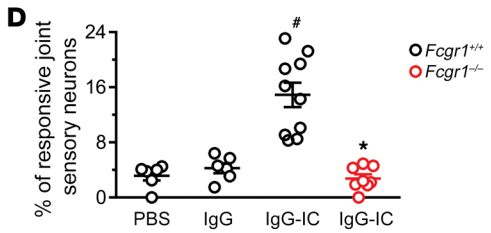

Figure 2. IgG-IC directly activates joint sensory neurons through FcγRI in vitro and in vivo. (**A**) Representative traces of Ca^{2+} responses evoked by antigen (Ag) alone (BSA), IgG-IC (1 μg/mL, 2 minutes), and capsaicin (CAP; 1 μM, 10 seconds) in joint-innervating (DiI-labeled) DRG neurons from *Fcgr1*$^{+/+}$ (left) and global *Fcgr1*$^{-/-}$ (right) mice. (**B**) Quantitative analysis showed that IgG-IC, but not Ag or antibody (Ab; anti-BSA) alone, evoked Ca^{2+} responses in a larger proportion of DiI-labeled joint sensory neurons from *Fcgr1*$^{+/+}$ mice than those from *Fcgr1*$^{-/-}$ mice. $^{*}P < 0.05$ vs. *Fcgr1*$^{+/+}$, $^{\#}P < 0.05$ vs. Ag; χ^2 test. Number of responsive neurons and total number tested are in parentheses. (**C**) Left: Representative DiI fluorescence (red) in L4 DRG neuronal cell bodies in *PirtCre-GCamp6* mice that were either *Fcgr1*$^{+/+}$ or *Fcgr1*$^{-/-}$, retrogradely labeled with ankle joint injection of DiI (2 mg/mL; 8 μL in saline). Right: GCAMP6 fluorescence (green) in the same fields before and after stimulation of the RF with the indicated stimuli. White arrows show DRG neurons from *Fcgr1*$^{+/+}$ mice exhibiting an increase in GCAMP6 fluorescence when the ankle was squeezed with blunt forceps and 4 minutes after IgG-IC (100 μg/mL; 10 μL) was injected into ankle joint cavity, but not after vehicle (PBS; 10 μL) or monomeric IgG (100 μg/mL; 10 μL) was injected. By contrast, little or no increase in GCAMP6 fluorescence was induced by IgG-IC in joint sensory neurons from *Fcgr1*$^{-/-}$ mice. Scale bar: 50 μm. (**D**) Quantitative analysis of Ca^{2+} responses to PBS (n = 6 mice), monomeric IgG (n = 6 mice), and IgG-IC (n = 10 mice) in joint sensory neurons of *Fcgr1*$^{+/+}$ mice and IgG-IC in *Fcgr1*$^{-/-}$ mice (n = 8 mice). $^{*}P < 0.05$ vs. *Fcgr1*$^{+/+}$, $^{\#}P < 0.01$ vs. PBS; 1-way ANOVA followed by Tukey's test.

FcγRI expressed in primary sensory neurons mediates IgG-IC–evoked nocifensive behaviors. Since FcγRI is a receptor for IgG-IC, we asked whether FcγRI mediates the acute pronociceptive effects of IgG-IC using global *Fcgr1*$^{-/-}$ mice. Global *Fcgr1*$^{-/-}$ mice exhibited normal basal mechanical sensitivity in the hind ankle and hind paw, and normal heat sensitivity in the hind paw, compared with *Fcgr1*$^{+/+}$ littermates (Figure 4, A–C). However, primary mechanical hypersensitivity in the ankle and secondary mechanical hypersensitivity in the hind paw upon i.a. injection of IgG-IC were significantly attenuated in *Fcgr1*$^{-/-}$ mice compared with *Fcgr1*$^{+/+}$ littermates (Figure 4, D–F). These findings suggest that FcγRI is necessary for IgG-IC–elicited acute nocifensive behaviors. Given that FcγRI is widely expressed in immune cells, we next investigated whether FcγRI-bearing immune cells are required for IgG-IC–induced joint hypernociception. In naive mice, i.a. injection of clodronate-laden liposomes, but not control liposomes, produced optimal depletion of synovial lining macrophages (31, 32), but did not affect basal mechanical or heat nociception 7 days after injection (Supplemental Figure 3, A–E). In addition, IgG-IC–evoked nocifensive behaviors were not significantly different between liposomal clodronate–treated mice and those treated with control liposomes (Figure 4, G and H). In mouse strains lacking either T cells (*Rag1*$^{-/-}$) or mast cells (*c-Kit*$^{W\text{-}sh/W\text{-}sh}$), we observed no significant differences in basal mechanical or thermal sensitivity (Supplemental Figure 3, F–K) or in IgG-IC–evoked nocifensive behaviors, compared with WT controls (Figure 4, I–L). Together, these results indicate that the pronociceptive effects of IgG-IC are mediated by FcγRI, but do not specifically require macrophages, lymphocytes, or mast cells. This left open the possibility that IgG-IC acts directly on FcγRI expressed on joint-innervating sensory neurons to elicit articular hypernociception via nonimmune modulation.

To more directly assess the potential involvement of neuronal FcγRI in the pronociceptive effects of IgG-IC, we generated a new mouse line bearing a conditional deletion allele of *Fcgr1* (*Fcgr1*$^{fl/fl}$) and crossed these mice with the *PirtCre* line to selectively omit *Fcgr1* expression from peripheral sensory neurons (Figure 5A). RT-qPCR and ISH analysis in *PirtCre Fcgr1*$^{fl/fl}$ mice confirmed that loss of *Fcgr1* expression specifically occurred in the DRG but not the spleen (Figure 5, B and C). Adult *PirtCre Fcgr1*$^{fl/fl}$ mice did not exhibit any abnormalities in basal sensitivity to mechanical or heat stimuli applied to the ankle or plantar skin of hind paws compared with WT littermate controls (Figure 5, D–F). However, *PirtCre Fcgr1*$^{fl/fl}$ mice exhibited less primary mechanical hypersensitivity in the ankle and less secondary mechanical hyperalgesia in the hind paw following i.a. injection of IgG-IC compared with *PirtCre* negative *Fcgr1*$^{fl/fl}$ control littermates (Figure 5, G–I). These results support the notion that neuronal FcγRI contributes to IgG-IC–evoked acute nocifensive behaviors in the naive state.

AIA upregulates FcγRI expression and function in DRG. We next used the well-established AIA murine model of RA, in which the provocative antigen is methylated bovine serum albumin (mBSA) (33, 34). We performed RT-qPCR on DRG tissue from WT mice subjected to this model to assay for alterations of *Fcgr1* mRNA expression. The *Fcgr1* mRNA expression level in the DRG was significantly greater in AIA mice than in vehicle control mice on days 1 and 3 after challenge (Figure 6, A and B). ISH analysis further revealed that, 3 days after challenge, a larger percentage of DRG neurons (including FB-labeled joint and non–FB-labeled non-joint sensory neurons) expressed *Fcgr1* mRNA in AIA mice compared with vehicle control–treated animals (Figure 6, C–E). Moreover, a greater proportion of *Fcgr1*$^{+}$ joint sensory neurons in AIA mice coexpressed CGRP as compared with those in control mice (Figure 6, B and F). To determine whether the function of FcγRI in joint sensory neurons was enhanced in the context of arthritis, we compared Ca^{2+} responses evoked by IgG-IC in DiI-labeled joint-innervating DRG neurons from control versus AIA mice using ratiometric Ca^{2+} imaging. As expected, the percentage of IgG-IC–responsive neurons was greater in AIA mice than in control animals (Figure 6G). These findings suggest that the expression and function of FcγRI in joint sensory neurons is significantly upregulated in the setting of AIA.

Genetic deletion of Fcgr1 attenuates arthritis pain in inflammatory arthritis models without obvious effects on joint inflammation. To explore whether FcγRI contributes to arthritis pain, we compared pain-related behaviors between *Fcgr1*$^{+/+}$ and *Fcgr1*$^{-/-}$ mice following AIA. Although both *Fcgr1*$^{+/+}$ and *Fcgr1*$^{-/-}$ mice developed primary mechanical hyperalgesia in the hind ankle, this effect was attenuated in global *Fcgr1*$^{-/-}$ compared with *Fcgr1*$^{+/+}$ mice (Figure 7A). Similarly, global *Fcgr1*$^{-/-}$ mice exhibited less secondary mechanical and thermal hyperalgesia in the hind paw than WT littermates over the course of AIA (Figure 7, B–D). However, no significant differences in joint swelling following AIA were observed between genotypes (Figure 7E). To further determine whether the apparent antihyperalgesic effects of *Fcgr1* knockout were attributable to a possible attenuation of joint inflammation, we measured the mRNA expression of a number of inflammatory mediators in the synovium 7 hours and 1 day after AIA. Among all the genes tested, AIA caused significant upregulation of *Il1b*, *Il6*, *Tnfa*, and *Cxcl1* in the synovium 7 hours after AIA (Supplemental Figure 4A). However, there were no significant differences in the alterations of the mRNA expression levels of these cytokines between genotypes. Similarly, the mRNA expression levels of *Mcp1* and *Mmp9*, in addition to *Il1b*, *Il6*, and *Cxcl1*, were upregulated to the same extent in both genotypes on day 1 after AIA (Supplemental Figure 4B). No significant changes in mRNA expression of other inflammatory mediators were observed in either genotype at 2 time points following AIA (Supplemental Figure 4B). On day 2 after AIA, joint IHC analysis showed that the marker for macrophages (CD68) was increased, but markers for T cells (CD3), neutrophils and monocytes (Ly6C/G), and mast cells (c-Kit) were not altered (Supplemental Figure 5, A and B). On day 4 after AIA, all assayed immune cell markers except c-Kit were increased (Supplemental Figure 6, A and B). However, none of the AIA-induced increases in any of these markers were significantly different between genotypes (Supplemental Figure 5, A and B, and Supplemental Figure 6, A and B). Similarly, joint histological H&E staining did not show significant differences in immune cell infiltration between genotypes on either day 2 (Supplemental Figure 5, C and D) or day 4 (Supplemental Figure 6, C and D) after AIA. In addition, we did not observe obvious immune cell infiltration within DRG on day 2 (data not shown) or 4 following AIA in either genotype (Supplemental Figure 7). Although FcγRI is apparently not involved in joint inflammation in the AIA model, it acts as a critical player in cartilage destruction during

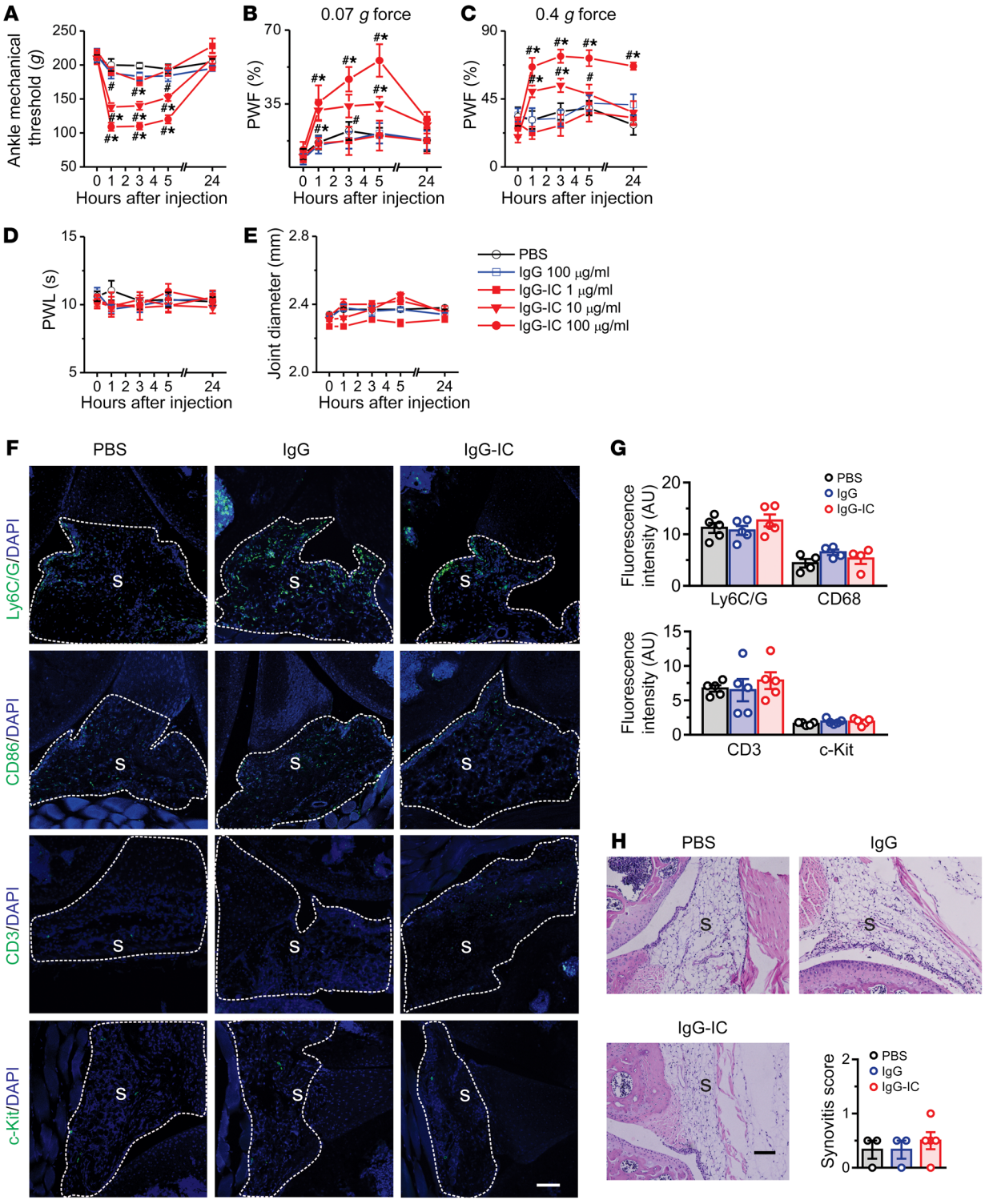

Figure 3. IgG-IC elicits acute articular hypernociception in naive mice. (**A**–**E**) Mice were injected intra-articularly (i.a.) with IgG-IC (1, 10, 100 μg/mL; 10 μL), monomeric IgG (100 μg/mL; 10 μL), or vehicle (PBS; 10 μL), and pain-like behaviors and joint diameter were evaluated over 1–24 hours. Injection of IgG-IC, but not monomeric IgG, reduced mechanical threshold in the ankle (**A**) and increased the frequency of paw withdrawal in response to application of 0.07 and 0.4 g force via a von Frey filament (**B** and **C**), but did not induce heat hyperalgesia (**D**) or visible joint swelling (**E**) in the ipsilateral paw, compared with vehicle. n = 8–10 mice per group; $^{*}P < 0.05$ vs. PBS, $^{\#}P < 0.05$ vs. before injection; 2-way ANOVA for repeated measures followed by Bonferroni's post hoc test. PWF, paw withdrawal frequency; PWL, paw withdrawal latency. (**F**) Representative sections of knee joints taken 1 hour after i.a. injection with either PBS, monomeric IgG, or IgG-IC and stained for Ly6C/G, CD68, CD3, or c-Kit. S, synovium. Scale bar: 200 μm. (**G**) Quantification showed no significant differences between treatment groups. n = 4–5 mice per group; $P > 0.05$; 1-way ANOVA followed by Tukey's test. (**H**) Representative sections of knee joint taken 1 hour after i.a. injection with PBS, monomeric IgG, or IgG-IC, stained with H&E, and scored for synovitis. S, synovium. Scale bar: 100 μm. No significant difference in synovitis score was observed between treatments. n = 3–4 mice per group; $P > 0.05$; 1-way ANOVA followed by Tukey's test.

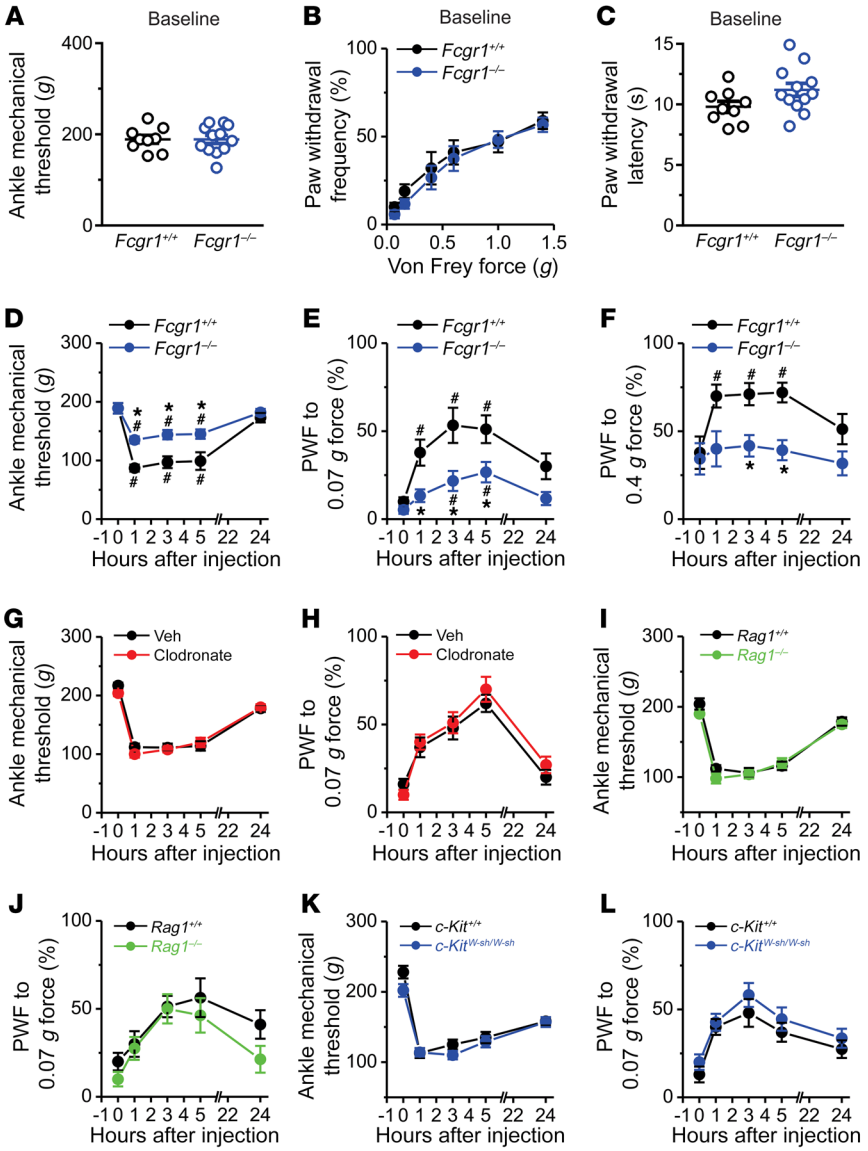

Figure 4. FcγRI mediates IgG-IC–induced acute joint nocifensive behaviors in mice. (**A**–**C**) Comparison of basal mechanical sensitivity to ankle press (**A**) and to plantar stimulation with von Frey filaments (**B**), and basal thermal sensitivity to plantar application of radiant heat (**C**), between *Fcgr1*$^{+/+}$ (n = 9 mice) and global *Fcgr1*$^{-/-}$ mice (n = 12 mice). $P > 0.05$; unpaired Student's t test or 2-way ANOVA for repeated measures followed by Bonferroni's post hoc test. (**D**–**F**) Global *Fcgr1*$^{-/-}$ mice (n = 12 mice) exhibited a higher mechanical threshold in the ankle (**D**) and lower paw withdrawal frequency (PWF) to 0.07 (**E**) and 0.4 g force (**F**) applied to the hind paw following i.a. injection of IgG-IC (100 μg/mL; 10 μL) compared with *Fcgr1*$^{+/+}$ control littermates (n = 9 mice). $^{*}P < 0.05$ vs. *Fcgr1*$^{+/+}$ controls, $^{\#}P < 0.05$ vs. before injection; 2-way ANOVA for repeated measures followed by Bonferroni's post hoc test. (**G** and **H**) Depletion of synovial macrophages with liposomal clodronate (5 mg/mL; 6 μL) had no significant effects on mechanical hyperalgesia in the ankle (**G**) or hind paw (**H**) in mice upon injection of IgG-IC, compared with liposomal control (Veh). n = 10 mice per group; $P > 0.05$; 2-way ANOVA for repeated measures followed by Bonferroni's post hoc test. (**I**–**L**) No significant differences were seen in IgG-IC–induced mechanical hyperalgesia in the ankle and hind paw in mice lacking T cells (*Rag1*$^{-/-}$) or mast cells (*c-Kit*$^{W\text{-}sh/W\text{-}sh}$) compared with WT controls. n = 10–11 mice per group; $P > 0.05$; 2-way ANOVA for repeated measures followed by Bonferroni's post hoc test.

AIA (18, 35). Thus, we next asked whether diminished AIA-associated hypernociception in global *Fcgr1*$^{-/-}$ mice is secondary to reduced cartilage destruction. However, TB/fast green staining analysis did not detect any obvious cartilage destruction on day 2 (Supplemental Figure 8, A–C) or 4 after AIA (Supplemental Figure 8, B–D). Together, these findings suggest that FcγRI contributes to arthritis pain through a mechanism that parallels joint inflammation and cartilage damage in the AIA model.

Given the importance of neuronal FcγRI in regulating the excitability of primary sensory neurons (28, 29), we next asked whether neuronally expressed FcγRI is involved in arthritis pain. In the AIA model, both male and female *PirtCre Fcgr1*$^{fl/fl}$ mice subjected to AIA showed significantly reduced primary mechanical hyperalgesia in the ankle (Figure 8A and Supplemental Figure 9A) and secondary mechanical hyperalgesia in the hind paw (Figure 8, B and C, and Supplemental Figure 9, B and C) compared with *Pirt-Cre* negative controls. However, there was no obvious difference between genotypes in either heat hyperalgesia in the hind paw (Figure 8D and Supplemental Figure 9D) or joint inflammation following AIA (Figure 8E and Supplemental Figure 9E).

CFA-induced arthritis is another animal model of inflammatory arthritis (36–38), in which serum levels of specific rheumatoid and immunological biomarkers, such as rheumatoid factor and IgG, are elevated (39). In this model, deletion of *Fcgr1* in sensory neurons significantly attenuated not only primary (Figure 8F) and secondary (Figure 8, G and H) mechanical hyperalgesia, but also secondary thermal hyperalgesia in the hind paw (Figure 8I). No significant difference in joint inflammation was observed between genotypes (Figure 8J). In addition, there was no difference between genotypes in the nocifensive behavior elicited by intraplantar injection of formalin, a short-term inflammatory agent (Figure 8, K and L). These findings suggest that neuronal FcγRI is critical to the development and maintenance of arthritis pain but is apparently not required for joint inflammation in the AIA or the CFA model. However, neuronal FcγRI is dispensable for some types of inflammatory pain.

Acute pharmacological blockade of peripheral FcγRI reverses arthritis pain in the AIA model. To circumvent potential confounding effects of genetic deletion of *Fcgr1*, we investigated whether acute pharmacological blockade of FcγRI at the periphery would

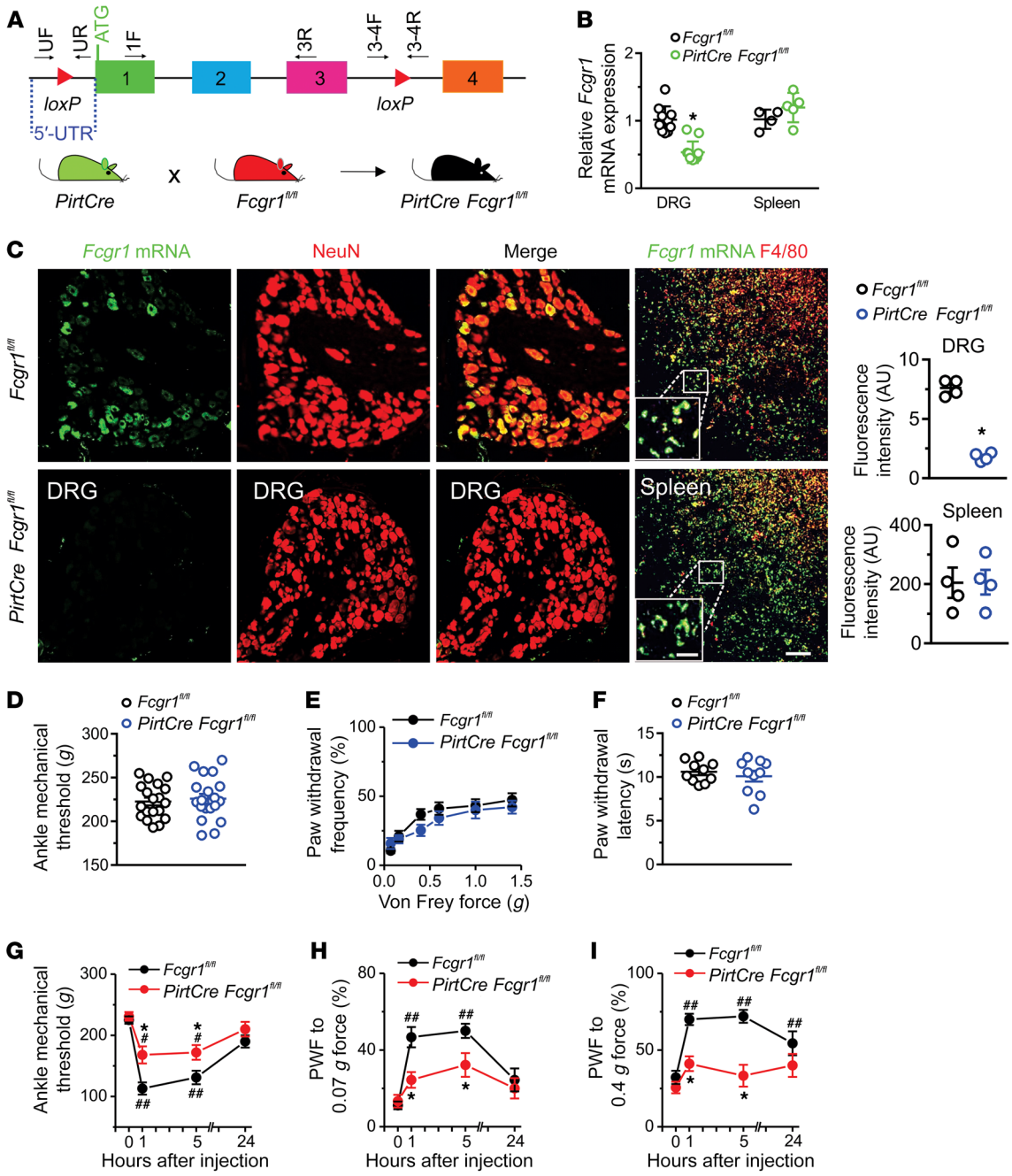

Figure 5. Neuronal FcγRI contributes to IgG-IC–induced acute nocifensive behaviors. (**A**) Strategy for generation of primary sensory neuron–selective *Fcgr1*-knockout mice. Two loxP sites were inserted 5′ to exon 1 and 3′ to exon 3 of the *Fcgr1* gene, respectively. Primers UF and UR and primers 3-4F and 3-4R, respectively, were used to confirm correct loxP insertions at each site. Deletion of the *Fcgr1* gene in primary sensory neurons was achieved by crossing of $Fcgr1^{fl/fl}$ mice with *PirtCre* mice. (**B**) RT-qPCR analysis using primers 1F and 3R from **A** revealed a significant reduction in *Fcgr1* mRNA expression in DRG tissue (n = 10–11 mice per group) but not in spleen of *PirtCre* $Fcgr1^{fl/fl}$ mice (n = 4–5 mice per group) compared with $Fcgr1^{fl/fl}$ controls. (**C**) Representative ISH image of DRG and spleen. Scale bar: 50 μm. Inset shows area of high-power magnification; scale bar: 20 μm. Quantification shows reductions in *Fcgr1* mRNA expression in DRG neurons (NeuN) but not in spleen macrophages (F4/80) of *PirtCre* $Fcgr1^{fl/fl}$ mice compared with $Fcgr1^{fl/fl}$ controls. n = 4 mice per group; $^{*}P < 0.05$ vs. $Fcgr1^{fl/fl}$ controls. For **B** and **C**, unpaired Student's t test was used. (**D**–**F**) No significant differences were observed between genotypes in basal mechanical sensitivity in the ankle (**D**) or hind paw (**E**), or in basal thermal sensitivity in the hind paw (**F**). n = 10–19 mice per group; $P > 0.05$; unpaired Student's t test or 2-way ANOVA for repeated measures followed by Bonferroni's post hoc test. (**G**–**I**) Time course of mechanical threshold in the ankle and paw withdrawal frequency (PWF) to 0.07 and 0.4 g force before and after i.a. injection of IgG-IC (100 μg/mL; 10 μL). n = 9 mice per group; $^{*}P < 0.05$ vs. $Fcgr1^{fl/fl}$ controls; $^{\#}P < 0.05$, $^{\#\#}P < 0.01$ vs. before injection; 2-way ANOVA for repeated measures followed by Bonferroni's post hoc test.

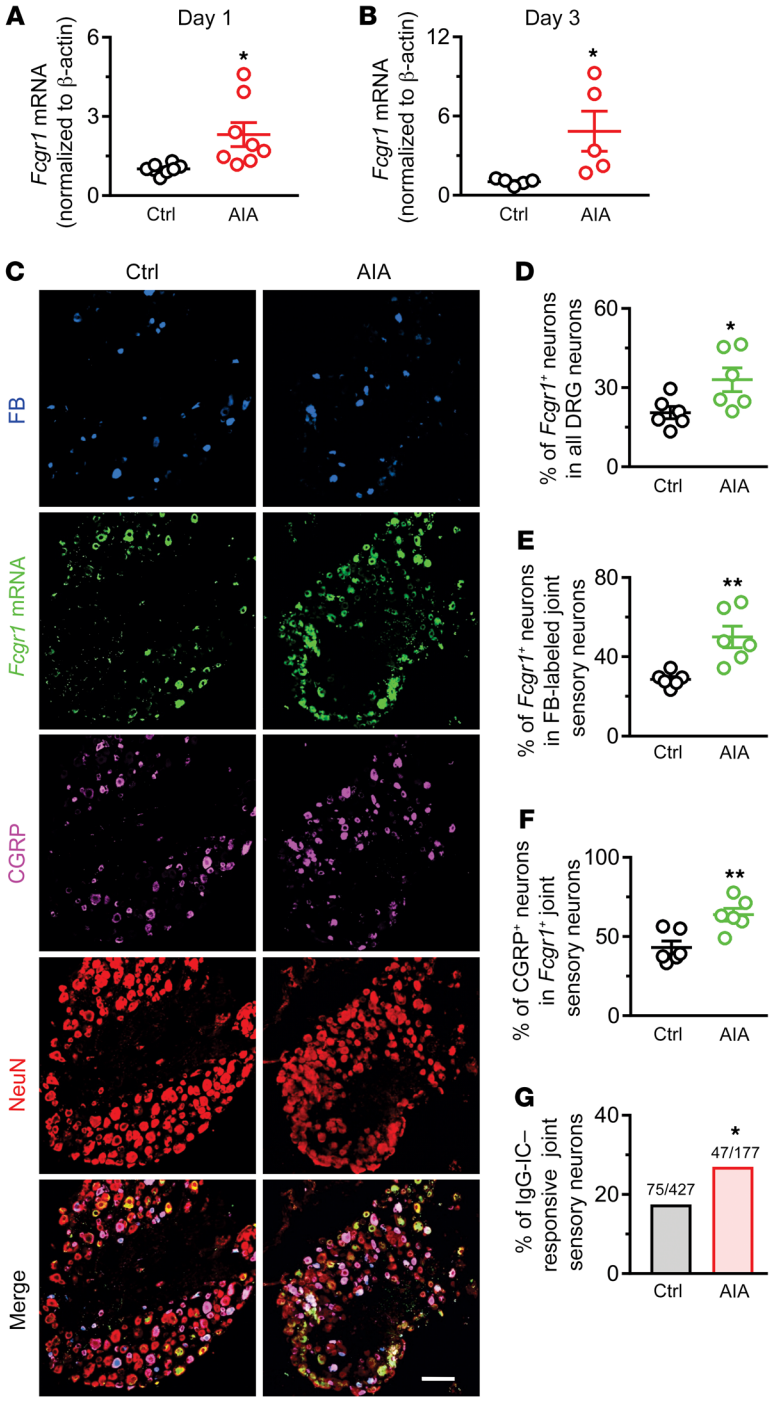

Figure 6. AIA upregulates the expression and function of FcγRI in mouse DRG neurons. (**A** and **B**) RT-qPCR analysis of *Fcgr1* mRNA expression normalized to that of *Actb* (β-actin) in the DRG of control (Ctrl) and AIA mice on days 1 (**A**; $n = 8$ mice per group) and 3 (**B**; $n = 5$ mice per group) after challenge. $^*P < 0.05$ vs. control; unpaired Student's *t* test. (**C**) Representative lumbar DRG ISH for *Fcgr1* and immunostaining for peripherin, NF200, and CGRP, and the merged image from control (Ctrl; $n = 6$) and AIA ($n = 6$) mice. DRG neurons innervating ankle joint were retrogradely labeled with FB. Scale bar: 50 μm. (**D**) Percentage of *Fcgr1*$^+$ neurons among all DRG neurons in control and AIA mice. (**E**) Percentage of *Fcgr1*$^+$ joint sensory neurons in control and AIA mice. (**F**) Percentage of CGRP$^+$ neurons among *Fcgr1*$^+$ joint sensory neurons in control and AIA mice. $n = 6$ mice per group; $^*P < 0.05$; $^{**}P < 0.01$ vs. control; unpaired Student's *t* test. (**G**) Quantitative analysis of Fura-2 Ca^{2+} imaging shows that a larger proportion of DiI-labeled joint sensory neurons from AIA mice responded to IgG-IC (1 μg/mL, 2 minutes) compared with those from control mice. $^*P < 0.05$ vs. control; χ^2 test. Numbers of responsive neurons divided by total number tested are noted above graphs.

attenuate arthritis pain. To test this possibility, we injected anti-CD64 monoclonal antibody (2.25 μg; 5 μL) or isotype control IgG2b into the inflamed ankle joint of WT mice once daily on days 1 and 2 after AIA (Figure 9A). In both male and female mice with established articular hypernociception, acute i.a. injection of anti-CD64 antibody produced rapid reductions in mechanical hyperalgesia in the inflamed ankle and in both mechanical and thermal hyperalgesia in the ipsilateral hind paw within 3 hours, but did not attenuate joint swelling (Figure 9, B–F, and Supplemental Figure 10, A–E). By contrast, i.a. injection of isotype control IgG2b had no such effects. Next, we further asked whether this analgesic effect of anti-CD64 is secondary to a reduction in joint inflammation using joint histological H&E staining. Neutralizing peripheral FcγRI did not significantly affect immune cell infiltration in the AIA joint compared with isotype control IgG2b (Figure 9, G and H). These findings suggest that local neutralization of FcγRI in the already inflamed joint reduces hyperalgesia through direct action on a neuronal target and/or via inhibition of ongoing local pronociceptive signaling, but not via the attenuation of inflammation.

Genetic deletion of Fcgr1 reduces AIA-induced hyperactivity of joint sensory afferents. Our recent study revealed that joint sensory afferents exhibited both abnormal hyperactivity and mechanical hypersensitivity in vivo following AIA (33). We therefore used an in vivo DRG recording preparation to determine whether deletion of *Fcgr1* would reduce hyperactivity of joint sensory afferents during AIA (33). Extracellular electrophysiological recordings were obtained on day 1 after challenge from DiI-labeled mechanosensitive sensory neurons with a receptive field (RF) within the vehicle- or mBSA-treated ankle. In *Fcgr1*$^{+/+}$ mice, a total of 29 (8 C and 21 Aδ fibers) and 36 (16 C and 20 Aδ fibers) joint-innervating DRG neurons were recorded from vehicle- and mBSA-challenged animals, respectively. In global *Fcgr1*$^{-/-}$ mice, a total of 21 (5 C and 16 Aδ fibers) and 28 (15 C and 13 Aδ fibers) joint sensory neurons were recorded from the vehicle and AIA group, respectively. All neurons tested had conduction velocities (CVs) within the ranges of C (≤1.5 m/s) or Aδ fibers (1.5–15 m/s). The mean CVs of C or Aδ fibers were similar between genotypes and treatments (Figure 10, A and B). Consistent with previous findings (33), all the tested DiI-labeled joint sensory neurons from vehicle-treated *Fcgr1*$^{+/+}$ mice were silent in the absence of exogenous stimuli, with no detectable spontaneous activity (SA) (Figure 10, C and D). In contrast, 10 (8 C and 2 Aδ fibers) of 36 (27.8%) joint sensory neurons

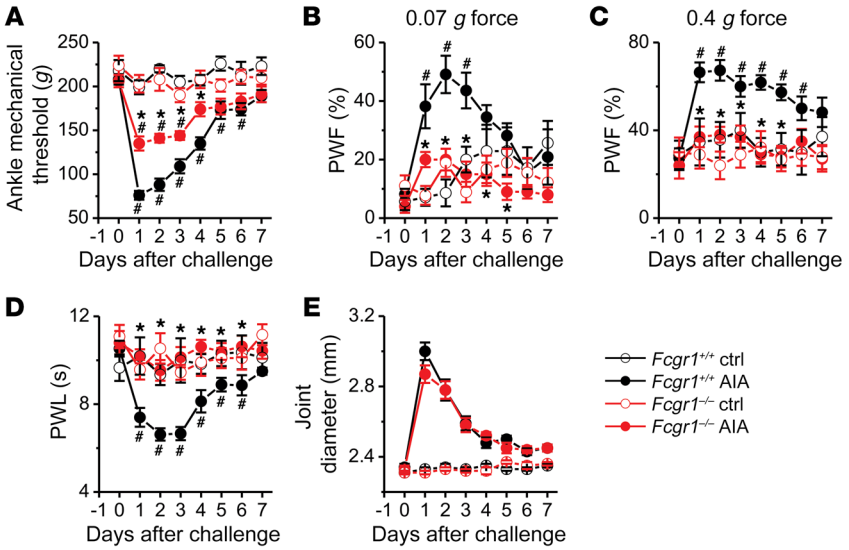

Figure 7. FcγRI modulates arthritis pain in the AIA model. Time course of mechanical threshold in the ankle (**A**), paw withdrawal frequency (PWF) in response to 0.07 g (**B**) and 0.4 g (**C**) force in the hind paw, paw withdrawal latency (PWL) to radiant heat in the hind paw (**D**), and ankle joint diameter (**E**) in *Fcgr1*$^{+/+}$ and global *Fcgr1*$^{-/-}$ mice after vehicle control (Ctrl) and mBSA (AIA) challenge. n = 7–11 mice per group; *P < 0.05 vs. *Fcgr1*$^{+/+}$, #P < 0.05 vs. day 0; 2-way repeated-measures ANOVA followed by Bonferroni's post hoc test.

in *Fcgr1*$^{+/+}$ mice with AIA exhibited SA. Similarly to vehicle-treated *Fcgr1*$^{+/+}$ mice, no SA was observed in any of 21 recorded joint sensory neurons from vehicle-treated *Fcgr1*$^{-/-}$ mice (Figure 10, C and D). Under AIA conditions, the incidence of SA was significantly lower in *Fcgr1*$^{-/-}$ mice (3 of 28 neurons; 10.7%; 2 C and 2 Aδ fibers) compared with *Fcgr1*$^{+/+}$ mice (Figure 10, C and D).

Since mechanical sensitization of joint sensory neurons likely represents a critical neuronal mechanism of mechanical hyperalgesia (33), we next asked whether FcγRI contributes to mechanical hypersensitivity of joint sensory neurons during AIA. To avoid the confounding effects of spontaneous firing, we exclusively focused on joint sensory afferents that did not exhibit SA. Under normal conditions, no mechanically evoked after-discharges were observed in either *Fcgr1*$^{+/+}$ or *Fcgr1*$^{-/-}$ mice. In the setting of AIA, 3 of 26 (11.5%; 2 C and 1 Aδ fibers) joint sensory neurons of *Fcgr1*$^{+/+}$ mice displayed after-discharges following punctate mechanical stimulation (10 or 20 mN; 2 seconds) of their RF, whereas no mechanically evoked after-discharges occurred in 25 joint sensory neurons recorded from *Fcgr1*$^{-/-}$ mice (Figure 10, E and F). We further compared mechanical sensitivity of joint sensory neurons that did not exhibit either SA or after-discharges between genotypes during AIA. Under arthritic conditions, the mean number of action potentials evoked by each mechanical force (5 mN to 40 mN) was significantly less in joint sensory neurons of *Fcgr1*$^{-/-}$ mice compared with those of *Fcgr1*$^{+/+}$ animals (Figure 10, G and H). These results indicate that FcγRI contributes to the sensitization of joint sensory neurons in the context of arthritis.

Discussion

Conventional wisdom has held that FcγRI, a common immune receptor for IgG-IC, is expressed exclusively in immune cells, where it plays a critical role in the regulation of various immune responses (13–16). However, we and others have previously reported evidence for the expression of FcγRI, but not FcγRII or FcγRIII, in a subpopulation of DRG neurons of rats and mice, respectively (27, 28). The results of our present study further challenge the traditional view of exclusive FcγRI function in immune cells by revealing that FcγRI is functionally and anatomically expressed in a subset of joint-innervating sensory neurons. Using ISH, we detected *Fcgr1* mRNA expression in joint-innervating DRG neurons of all size categories, including both peptidergic and nonpeptidergic neurons. We also demonstrated that neuronal FcγRI activation is sufficient to drive joint sensory neuron firing, a conclusion supported by our in vivo and in vitro assays showing that IgG-IC can directly activate joint sensory neurons at their somata and peripheral terminals in a manner dependent on neuronal FcγRI.

A second advance achieved by this study is the revelation of a novel role for FcγRI, and for neuronally expressed FcγRI in particular, in modulating joint pain in both naive and arthritis states. Acute pharmacological blockade, global deletion, and conditional deletion of *Fcgr1* in primary sensory neurons each effectively alleviated the pronociceptive action of IgG-IC under naive conditions and arthritis pain in the AIA and CFA models. Strikingly, these analgesic effects seem to be dissociable from effects on joint inflammation. Therefore, we suggest that peripheral FcγRI signaling, specifically in primary sensory neurons, contributes to arthritis pain through a mechanism that parallels inflammation and other pathological processes.

Sensitization of nociceptive joint sensory fibers likely represents a key mechanism in arthritis pain. In a recent study, we found that AIA enhances the in vitro excitability of joint-innervating DRG neurons (33). In addition, in vivo extracellular electrophysiological recordings on intact DRG showed that AIA causes spontaneous sensory neuronal activity and increases the responses of joint sensory neurons to mechanical stimulation (33). Enhanced mechanical sensitivity of joint sensory neurons might provide a peripheral neural basis for the behavioral signs of primary mechanical allodynia and/or hyperalgesia that accompany RA. Moreover, increased peripheral sensory afferent input might trigger ongoing spontaneous pain in arthritis and contribute to the development and maintenance of central sensitization. In the present study, we revealed that genetic deletion of *Fcgr1* reduced both the incidence of abnormal activity of joint sensory fibers and mechanical hypersensitivity of joint sensory neurons after AIA, suggesting that FcγRI is necessary to sustain aberrant peripheral nociceptive activity in the context of this model of arthritis. Given

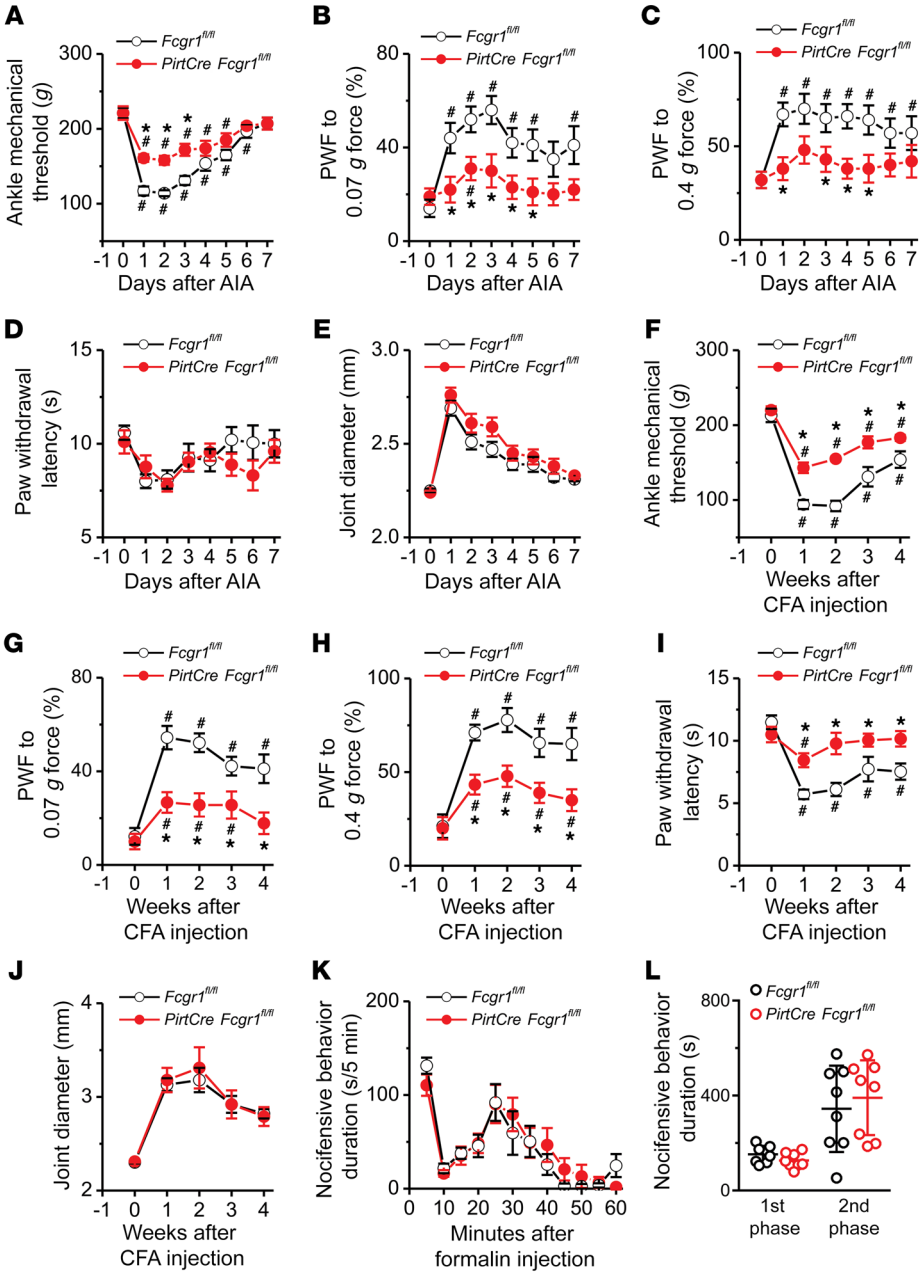

Figure 8. Neuronal FcγRI mediates arthritis pain in the AIA and CFA models. (**A**–**E**) Time course of ankle mechanical threshold (**A**), paw withdrawal frequency (PWF) to 0.07 g (**B**) and 0.4 g force (**C**), paw withdrawal latency to radiant heat (**D**), and ankle joint diameter (**E**) of male mice following AIA in *PirtCre Fcgr1*$^{fl/fl}$ mice and *Fcgr1*$^{fl/fl}$ control littermates. $n = 10$ mice per group; $^{*}P < 0.05$ vs. *Fcgr1*$^{fl/fl}$ controls, $^{\#}P < 0.05$ vs. day 0; 2-way repeated-measures ANOVA followed by Bonferroni's post hoc test. (**F**–**J**) Ankle mechanical threshold (**F**), PWF to 0.07 g (**G**) and 0.4 g force (**H**), paw withdrawal latency to radiant heat (**I**), and ankle joint diameter (**J**) in male *Fcgr1*$^{fl/fl}$ and *PirtCre Fcgr1*$^{fl/fl}$ mice after injection of CFA (5 μL) into the ankle joint. $n = 10$ mice per group; $^{*}P < 0.05$ vs. *Fcgr1*$^{fl/fl}$ controls, $^{\#}P < 0.05$ vs. week 0; 2-way repeated-measures ANOVA followed by Bonferroni's post hoc test. (**K** and **L**) Total duration of pain-related behavior during the first (1–10 minutes) and second phases (11–60 minutes) after intraplantar injection of formalin (5%; 20 μL) in *Fcgr1*$^{fl/fl}$ and *PirtCre Fcgr1*$^{fl/fl}$ mice (both sexes). $n = 8$ mice per group; $P > 0.05$ vs. *Fcgr1*$^{fl/fl}$ controls; 1-way repeated-measures ANOVA followed by Bonferroni's post hoc test.

that FcγRI is widely expressed in immune cells and is of critical importance to immune modulation, proinflammatory cytokines released within the damaged tissue under arthritic conditions might be important mediators of this process. However, our present study and reports from other groups suggest that FcγRI is not a major driver of joint inflammatory processes in the AIA model (18, 20). Therefore, it is plausible that FcγRI promotes AIA-induced hyperactivity of joint sensory afferents through a mechanism that operates in parallel with immune modulation. The expression and function of FcγRI in joint sensory afferents raise the possibility that neuronal FcγRI might be directly involved in this process. In our previous study, we demonstrated that neuronal FcγRI is functionally coupled to TRPC3 via the Syk/PLC/IP3 pathway to regulate the excitability of DRG neurons (29). Further work is therefore warranted to explore whether TRPC3 is involved in FcγRI-mediated arthritis pain. Neuronal FcγRI may also contribute to AIA-associated joint pain indirectly, by modulating the release of pain mediators such as CGRP and substance P from joint sensory neurons. Indeed, in cultured DRG neurons, FcγRI has been reported to mediate IgG-IC–induced substance P release (27), which may in turn activate or sensitize joint sensory neurons through its own receptor in a paracrine or autocrine manner (40). This might account for AIA-induced sensitization of joint sensory neurons that do not express FcγRI. Further investigation using sensory neuron subtype–specific *Fcgr1*-knockout mice will be necessary to assess these potential cell-autonomous and non–cell-autonomous roles of neuronal FcγRI.

RA is characterized by the accumulation of IgG-IC at the affected joint and the production of autoantibodies (41). Much attention has been focused on the role of IgG-IC/FcγRI signaling

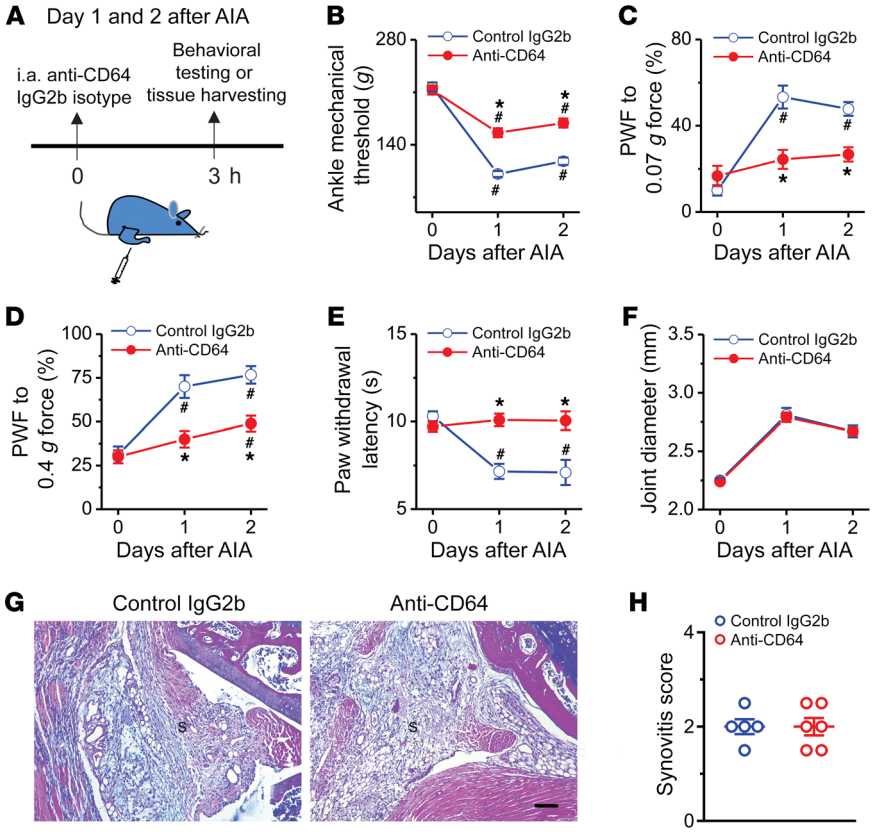

Figure 9. Acute pharmacological blockade of FcγRI attenuates AIA-associated pain in male mice. (**A**) Experimental schematic indicating once-daily injection of anti-CD64 (2.25 μg; 5 μL) or IgG2b isotype control (2.25 μg; 5 μL) into knee (for histology) or ankle cavity (for behavioral testing) of mice on days 1 and 2 after AIA. Pain-related behaviors were measured within 3 hours after each injection. (**B**–**F**) Effects of repeated daily i.a. injection of anti-CD64 or IgG2b isotype control on mechanical threshold in the ankle (**B**), paw withdrawal frequency (PWF) in response to 0.07 g (**C**) and 0.4 g force (**D**), paw withdraw latency to radiant heat (**E**), and ankle joint diameter (**F**) in the mice with AIA. $n = 9$ mice per group; $^{*}P < 0.05$ vs. control IgG2b isotype, $^{\#}P < 0.05$ vs. day 0; 2-way ANOVA for repeated measures followed by Bonferroni's post hoc test. (**G**) H&E staining assessment of synovitis in the inflamed knee joint of AIA mice treated with IgG2b isotype control ($n = 5$ mice) or anti-CD64 ($n = 6$ mice). S, synovium. Scale bar: 100 μm. (**H**) Quantification showed no difference in synovitis score between treatment groups. $P > 0.05$, unpaired Student's t test.

in RA pathogenesis (18, 35, 42, 43). Yet little is known of its contribution to joint pain that accompanies this disorder. In this study, 4 orthogonal and complementary lines of evidence support the hypothesis that IgG-IC/FcγRI signaling, particularly in neurons, is necessary and sufficient to mediate joint pain via a mechanism that is at least to some extent dissociable from joint inflammation.

First, in naive mice, exogenous application of IgG-IC elicited joint nociceptive behaviors whereas the pronociceptive effect of IgG-IC was diminished in mice lacking *Fcgr1*. It is conceivable that IgG-IC/FcγRI signaling could induce joint pain hypersensitivity by mobilizing immune cells and inflammatory responses. We did not, however, observe any obvious visual or histological signs of joint inflammation at early stages after IgG-IC injection. Moreover, RT-qPCR analysis did not detect any acute alterations in the mRNA expression levels of various inflammatory mediators in the synovium following IgG-IC injection. In addition, depletion or deletion of immune cells had no impact on the pronociceptive action of IgG-IC. Based on the time scale of rapid modulation of neuronal activity by ligand (minutes to hours), the transient changes in pain behavior after i.a. injection of IgG-IC are likely mediated by neuronal activation. The present findings, showing that IgG-IC had a direct action on neuronal activity in vivo and in vitro, thus support the view that IgG-IC may directly activate joint sensory neurons though FcγRI to elicit joint pain hypersensitivity in the naive state. The involvement of neuronally expressed FcγRI was further validated by use of our newly generated conditional *Fcgr1*-knockout mice, in which *Fcgr1* is specifically deleted in primary sensory neurons. Conditional deletion of *Fcgr1* remarkably suppressed IgG-IC–evoked nocifensive behaviors in naive mice.

Second, FcγRI expression and function were upregulated within DRG in the AIA model. In RA patients, FcγRI is expressed de novo in the synovium (44), and its expression level in neutrophils, monocytes, and synovial macrophages is upregulated (19, 45, 46). The mechanisms underlying the upregulation of FcγRI signaling require further study. It is probably due to the activation of a signaling cascade of inflammatory cytokines during arthritis, which upregulates FcγRI expression (47). In addition, cytokines may enhance the function of FcγRI by increasing the binding of IgG-IC to FcγRI (48). In this study, we revealed that a larger proportion of FcγRI-expressing joint sensory neurons displayed CGRP immunopositivity after AIA. Activation of neuronal FcγRI may result in more CGRP release from joint sensory afferents under arthritic conditions. The release of CGRP has been implicated in the generation of pain in certain arthritis models (49, 50). Therefore, it is possible that neuronal FcγRI contributes to arthritis pain through a mechanism involving neurogenic inflammation. However, deletion of neuronal *Fcgr1* attenuated mechanical hyperalgesia but not joint swelling during AIA, suggesting that FcγRI expressed on peptidergic sensory neurons may signal hyperalgesia, but may not promote neuroinflammatory responses via neurogenic inflammation. Given that activation of sensory neurons is able to regulate innate and adaptive immunity (51), however, we cannot completely rule out a possible immune contribution of neuronal FcγRI to RA pain, especially in the late phase.

Third, global deletion of *Fcgr1* attenuated arthritis pain in the AIA model. These inhibitory effects are unlikely to be secondary to the reductions in joint inflammation for several reasons. Previous studies have demonstrated that FcγRI is not essential for

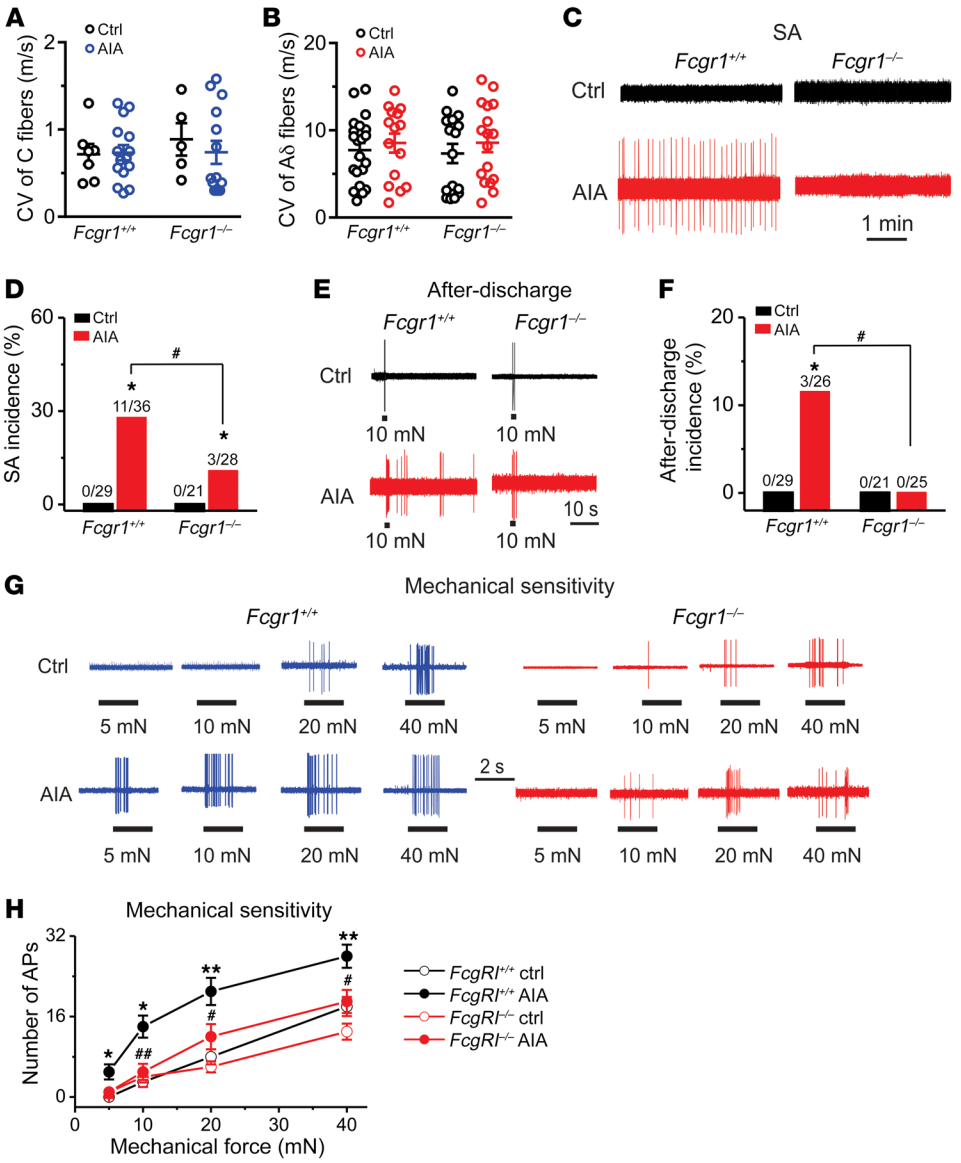

Figure 10. FcγRI contributes to hyperactivity of joint sensory neurons following AIA. (**A** and **B**) Distribution of the recorded C (**A**) and Aδ (**B**) fibers innervating the ankle of *Fcgr1*$^{+/+}$ and *Fcgr1*$^{-/-}$ mice 1 day after vehicle control (Ctrl) or mBSA (AIA) challenge. No significant difference in CV was seen between treatments or genotypes. $P > 0.05$, 2-way ANOVA followed by Bonferroni's post hoc test. (**C**) Representative traces of abnormal spontaneous activity (SA) were recorded in DiI-labeled joint sensory neurons of mice. (**D**) Global *Fcgr1*$^{-/-}$ mice exhibited lower incidence of SA at day 1 after AIA. $^{*}P < 0.05$ vs. controls, $^{\#}P < 0.05$ vs. *Fcgr1*$^{+/+}$ mice; χ^2 test. Number of neurons tested is noted above graphs. (**E**) Responses of joint sensory neurons in *Fcgr1*$^{+/+}$ and *Fcgr1*$^{-/-}$ mice to a 2-second, 10-mN mechanical stimulus delivered via a 100-μm probe in control (Ctrl) and AIA mice. (**F**) Prevalence of mechanically evoked after-discharges in joint sensory neurons of *Fcgr1*$^{+/+}$ and *Fcgr1*$^{-/-}$ mice on day 1 after challenge. $^{*}P < 0.05$ vs. controls, $^{\#}P < 0.05$ vs. *Fcgr1*$^{+/+}$ mice; χ^2 test. Number of neurons tested is noted above graphs. (**G**) Representative responses of joint sensory neurons in *Fcgr1*$^{+/+}$ and *Fcgr1*$^{-/-}$ mice to mechanical stimulation (2 seconds in duration) of their RF with von Frey filaments (100 μm tip diameter) at the indicated bending forces on day 1 after challenge. (**H**) The mean number of action potentials evoked by mechanical stimuli in joint sensory neurons from *Fcgr1*$^{+/+}$ (Ctrl: 29 neurons; AIA: 23 neurons) and *Fcgr1*$^{-/-}$ mice (Ctrl: 21 neurons; AIA: 25 neurons) on day 1 after AIA. $^{*}P < 0.05$, $^{**}P < 0.01$ vs. controls; $^{\#}P < 0.05$, $^{\#\#}P < 0.01$ vs. *Fcgr1*$^{+/+}$; 2-way repeated-measures ANOVA followed by Bonferroni's post hoc test.

inflammatory processes in this model (18, 20). Moreover, in line with previous studies (52), our qPCR assay revealed an upregulation of inflammatory mediators in the inflamed synovium of mice with AIA. Yet the extent of the upregulation was similar between WT and global *Fcgr1*$^{-/-}$ mice. IHC staining and joint histological analysis further showed that immune cell infiltration in the AIA joint was not different between genotypes. Although FcγRI has been implicated in cartilage destruction in the AIA model (18, 35), we did not observe obvious histological changes in cartilage in the inflamed joints at the early phase of AIA (i.e., days 2 and 4). One possible explanation for this discrepancy is that obvious cartilage destruction may only occur at the later time points (i.e., day 7) in the AIA model (18). Thus, our findings argue against the possibility that global deletion of *Fcgr1* attenuated arthritis pain primarily via reductions of cartilage destruction.

Fourth, acute blockade of FcγRI at the periphery, achieved with local injection of anti-CD64 antibody, markedly attenuated established arthritis pain, but not joint swelling, in the AIA model. Joint histological analysis further confirmed that acute pharmacological inhibition of FcγRI had no detectable impact on immune cell infiltration into the inflamed synovium. It is therefore likely that the analgesic effect of neutralizing FcγRI is due to direct action on a neuronal target and/or inhibition of ongoing local pronociceptive signaling, and not to the attenuation of joint inflammation.

Although RA pain is often thought to be of inflammatory origin, joint inflammation alone does not entirely account for arthritis pain (5, 6). The present study sheds light on a novel mechanism that might contribute to RA-associated pain. We suggest that IgG-IC accumulated in the inflamed joint is sufficient to directly activate and sensitize joint sensory neurons through neuronal FcγRI to evoke joint pain. Since no single experimental model of arthritis recapitulates all aspects of human RA (53), our data from the AIA and CFA models might not be completely generalizable to other models. We also cannot exclude the contributions of neuronal FcγRI to inflammation-related events beyond the sensitivity of our histological and biochemical assays. In addition, our data do not rule out the involvement of other central and peripheral noninflammatory mechanisms in arthritis pain. Nevertheless, this pro-

posed new location and role for IgG-IC/FcγRI signaling might be especially relevant to joint pain that occurs prior to the detectable onset of inflammation or that which persists even after apparently successful reversal of joint inflammation. Critical assessment of neuronal FcγRI contributions to additional arthritis models and future translational studies are therefore warranted to define the biological relevance of our findings, and to determine whether neuronal FcγRI merits consideration as a therapeutic target for the treatment of RA pain.

Methods

Supplemental Methods are available online with this article; https://doi.org/10.1172/JCI128010DS1.

Animals. Animals were housed under a 12-hour light/12-hour dark cycle with ad libitum access to food and water. Male mice used in the study were 2–3 months of age and weighed 20–30 g. In some experiments, female mice were also used as indicated. Breeders of T or B cell–deficient *Rag1*$^{-/-}$ mice and mast cell–deficient *c-Kit*$^{W\text{-}sh/W\text{-}sh}$ mice were obtained from The Jackson Laboratory. Breeders of global *Fcgr1*$^{-/-}$ mice and *PirtCre-GCamp6* mice were provided by Sjef Verbeek (Leiden University Medical Center, Leiden, The Netherlands) and Xinzhong Dong (Johns Hopkins University, Baltimore, Maryland, USA), respectively. Littermates were generated by interbreeding of heterozygotes on the C57BL/6 background.

Generation of Fcgr1$^{fl/fl}$ *mice*. *Fcgr1*$^{fl/fl}$ mice were generated using CRISPR/Cas9 genome editing. Two loci in the *Fcgr1* gene were targeted for loxP site insertion, one 283 nucleotides upstream of exon 1 and another 223 nucleotides downstream of exon 3, more than 200 bp away from splice donor or acceptor sequences. The loxP sites were designed close enough to one another (<2.5 kb) to allow efficient Cre-mediated recombination. Guide RNA (gRNA) sequences were designed using the CRISPR Design Tool (CRISPR.mit.edu), to target these loci within the *Fcgr1* gene while minimizing off-target mutations. CRISPR RNAs (crRNAs) corresponding to each gRNA (5′-CAGUAAACCCUGAAAGAGUGGUUUUAGAGCUAUGCUGUUUUG-3′ for the gRNA upstream of exon 1 and 5′-AUCCCCCGCUGGACCAGUUUGUUUUAGAGCUAGGCUGUUUUG-3′ for the gRNA downstream of exon 3) were synthesized commercially (Dharmacon). Two corresponding homology repair templates (HRTs) containing a loxP site with adjacent restriction sites and flanked on each side by 36 nucleotides of target sequence homology were generated by PCR (54), using a loxP site–containing plasmid (pBS-loxP plasmid, gift of Randall Reed, Johns Hopkins University) as a template and the following primers: HRT upstream of exon 1: forward, 5′-ATTCAGGCTATCAGAGCTACAGTAAACCCTGAAAGAGCGGTGGCGGCCGCTCTAGA-3′; reverse, 5′-GCTACCATGACTAGCTACATATCCCTCCCACCTCACTCCTGCAGCCCGGGGGATCC-3′; loxP insertion at the downstream of exon 3: forward, 5′-AGGCCCTATTTGCCTGCAGCATCCCCCGCTGGACCAGCGGTGGCGGCCGCTCTAGA-3′; reverse, 5′-GAGCCCGGGATTTTTGGGTGACACTGTCACCCAAACTCCTGCAGCCCGGGGGATCC-3′. crRNAs, *trans*-activating crRNA (trRNA), Cas9 protein (provided by Johns Hopkins University Transgenic Mouse Core Facility), and the double-stranded HRT DNAs were microinjected into C57BL/6 mouse zygotes and implanted into pseudopregnant females by the Johns Hopkins University School of Medicine Transgenic Mouse Core Facility. Tail genomic DNA from founders and offspring was genotyped using 2 sets of primers (for loxP insertion at 5′-UTR of exon 1: forward [UF], 5′-GATCTCTGTGAGGTCAAGGCT-3′; reverse [UR], 5′-CCTCCCAAGTGCTAGGATTAT-3′; for loxP insertion at the downstream of exon 3: forward [3-4F], 5′-GTCAAATCAGGTCAGACAGCT-3′; reverse [3-4R], 5′-AGAACTGCTGTGGGTGAAGCT-3′), as shown in Figure 5A. Only 1 of 26 founders possessed 2 loxP sites inserted to the same allele. This founder was then backcrossed 10 generations against C57BL/6 mice to eliminate off-target mutations. All the offspring developed normally except that about 10 of them obtained during the first 3–5 generations of backcross exhibited spontaneous turning behavior and were excluded from behavior studies. To generate sensory neuron–specific *Fcgr1*-knockout mice (*PirtCre Fcgr1*$^{fl/fl}$), *Fcgr1*$^{fl/fl}$ mice were crossed onto *PirtCre* mice to achieve *Fcgr1* deletion in peripheral sensory neurons. The efficiency of *Fcgr1* mRNA deletion in DRG was confirmed by quantitative real-time PCR using 1 set of primers (Figure 5A; forward [1F], 5′-CAGCCTCCATGGGTCAGT-3′; reverse [3R], 5′-TGAAAACTGGCCTCTGGGAT-3′).

Preparation of IgG-IC. IgG immune complex (IgG-IC) was formed by incubation of BSA (10 μg/mL; Sigma-Aldrich) and anti-BSA IgG (5 mg/mL; MP Biomedicals) at the mass ratio of 1:2 for 1 hour at 37°C as described previously (55). The IgG-IC was then diluted to the concentrations of 1, 10, and 100 μg/mL. Given that the estimated molecular mass of immune complexes is typically around 650–850 kDa (56), the molar concentration of 1 μg/mL is equivalent to 1.2–1.5 nM. Doses were chosen based on our pilot studies and other reports (57).

Intra-articular injection of IgG-IC and anti-FcγRI (CD64) antibody. IgG-IC (1, 10, 100 μg/mL; 10 μL) was injected into the right knee (for joint histology and real-time PCR on synovial tissue) or ankle (for behavioral testing) joint cavity of naive mice. The same amounts of monomeric IgG and PBS served as controls. Pain-related behaviors and ankle diameter were measured 1–24 hours after injection. Since the concentration of 100 μg/mL is within the range of IgG-IC accumulated in the serum in RA patients (57), this concentration was chosen throughout this study. In some experiments, either rat anti–mouse FcγRI monoclonal antibody (2.25 μg in 10 μL saline; R&D Systems) or isotype control (monoclonal rat IgG2b; R&D Systems) was injected into the right knee (for joint histology) or ankle (for behavioral testing) of mice on days 1 and 2 after AIA. Pain-related behaviors and joint swelling were assessed over the ensuing 3 hours.

Retrograde labeling of ankle joint sensory afferents. For in vivo and in vitro studies, DRG cell bodies with their afferent fibers innervating ankle joints were identified by the presence of a retrogradely transported red fluorescent dye, DiI (Sigma-Aldrich). DiI was injected into the right ankle (2.5 mg/mL; 8 μL in 25% ethanol) at least 1 week before harvesting. Since our pilot study showed that DiI was not compatible with ISH assay, fast blue (FB; 8 μL; 1% in saline; Polysciences Inc.) was alternatively injected to the ankle cavity at least 2 weeks before harvesting.

In situ hybridization. SP6 transcribed antisense and T7 transcribed sense control probes were synthesized from mouse *Fcgr1* (NM_010186) cDNA clone (MR225268, OriGene) using 1 set of primers (forward, 5′-ATTTAGGTGACACTATAGAATCCTCAATGCCAAGTGACCC-3′; reverse, 5′-GCGTAATACGACTCACTATAGGGCGCCATCGCTTCTAACTTGC-3′). The antisense probe was designed to target exons 1–6 of the mouse *Fcgr1* gene. The probes were then labeled using a digoxigenin (DIG) RNA labeling kit (Roche 11277073910) according to the manufacturer's instructions. Prehybridization, hybridization, and washing were performed on DRG and spleen sections using standard methods (58). The temperatures for prehybridization/hybridiza-

tion and for washing were 60°C and 62°C, respectively. To combine ISH with IHC, tissue sections were incubated with sheep anti-DIG antibody (Supplemental Table 2) and subjected to the standard IHC protocol as above.

Knee histology. Hind knee joints from mice were postfixed in 4% paraformaldehyde for 48 hours, decalcified in 10% EDTA (Sigma-Aldrich) for 3–4 weeks, and then dehydrated in ethanol and embedded in paraffin. Sections (5 μm) were cut and stained with H&E or toluidine blue (TB)/fast green and scored by the evaluators in a blinded manner. Three sections per knee joint at different depths were analyzed for synovitis on a scale from 0 (normal) to 3 (severe) (59) and for cartilage damage on a scale from 0 (normal) to 6 (bone loss, remodeling, deformation) (60). The score per knee was averaged.

Statistics. Data are presented as means ± SEM. Two-tailed Student's *t* test was used to test the significance of differences between 2 groups. Comparisons for multiple groups or multiple time points were carried out using a 1-way or 2-way ANOVA for random measures or repeated measures followed by Bonferroni's or Tukey's post hoc test comparisons. Comparisons of proportions were made by χ^2 test. *P* less than or equal to 0.05 was considered significant. Group sizes and the type of statistical tests used for each comparison are noted in each figure legend.

Study approval. All animal experimental procedures were approved by the Institutional Animal Care and Use Committee of Johns Hopkins University School of Medicine and were in accordance with the guidelines provided by the NIH and the International Association for the Study of Pain.

Author contributions

LQ conceived the project, designed the experiments, conducted behavioral tests, in vivo and in vitro calcium imaging, and in vivo electrophysiological experiments, analyzed the data, and wrote the manuscript. LW performed IHC and joint histology staining, quantitative RT-PCR, and in situ hybridization experiments. XJ and SMJ carried out quantitative RT-PCR. QZ carried out in vivo calcium imaging. TC performed joint histology staining. YL carried out behavioral tests. RR and HK assisted with gRNA and homology-directed repair vector design and founder genotyping. MJC and XD facilitated experimental design and analysis and revised the manuscript.

Acknowledgments

We thank Sjef Verbeek for providing global *Fcgr1*$^{-/-}$ mice. We thank Daniel Bennett, Neil Bolduc, and Luke Davis for mouse colony maintenance. We also thank the Transgenic Mouse Core Facility at Johns Hopkins University School of Medicine for assistance with generating *Fcgr1*$^{fl/fl}$ mice. This work is supported by NIH R01 grant AR072230 (to LQ), a Johns Hopkins Blaustein Pain Research Grant (to LQ), and the Neurosurgery Pain Research Institute at Johns Hopkins University.

Address correspondence to: Lintao Qu, Neurosurgery Pain Research Institute, Johns Hopkins School of Medicine, 725 N. Wolfe Street, Baltimore, Maryland 21205, USA. Phone: 410.955.3760; Email: lqu4@jhmi.edu.

1. McInnes IB, Schett G. The pathogenesis of rheumatoid arthritis. *N Engl J Med*. 2011;365(23):2205–2219.
2. Redlich K, Smolen JS. Inflammatory bone loss: pathogenesis and therapeutic intervention. *Nat Rev Drug Discov*. 2012;11(3):234–250.
3. Durham CO, Fowler T, Donato A, Smith W, Jensen E. Pain management in patients with rheumatoid arthritis. *Nurse Pract*. 2015;40(5):38–45.
4. Walsh DA, McWilliams DF. Mechanisms, impact and management of pain in rheumatoid arthritis. *Nat Rev Rheumatol*. 2014;10(10):581–592.
5. Courvoisier N, et al. Prognostic factors of 10-year radiographic outcome in early rheumatoid arthritis: a prospective study. *Arthritis Res Ther*. 2008;10(5):R106.
6. Studenic P, Radner H, Smolen JS, Aletaha D. Discrepancies between patients and physicians in their perceptions of rheumatoid arthritis disease activity. *Arthritis Rheum*. 2012;64(9):2814–2823.
7. Koop SM, ten Klooster PM, Vonkeman HE, Steunebrink LM, van de Laar MA. Neuropathic-like pain features and cross-sectional associations in rheumatoid arthritis. *Arthritis Res Ther*. 2015;17:237.
8. Lee YC, et al. Pain persists in DAS28 rheumatoid arthritis remission but not in ACR/EULAR remission: a longitudinal observational study. *Arthritis Res Ther*. 2011;13(3):R83.
9. Lee YC, et al. Subgrouping of patients with rheumatoid arthritis based on pain, fatigue, inflammation, and psychosocial factors. *Arthritis Rheumatol*. 2014;66(8):2006–2014.
10. Wigerblad G, et al. Autoantibodies to citrullinated proteins induce joint pain independent of inflammation via a chemokine-dependent mechanism. *Ann Rheum Dis*. 2016;75(4):730–738.
11. Ellsworth JL, et al. Recombinant soluble human FcgammaR1A (CD64A) reduces inflammation in murine collagen-induced arthritis. *J Immunol*. 2009;182(11):7272–7279.
12. Grevers LC, de Vries TJ, Everts V, Verbeek JS, van den Berg WB, van Lent PL. Immune complex-induced inhibition of osteoclastogenesis is mediated via activating but not inhibitory Fcγ receptors on myeloid precursor cells. *Ann Rheum Dis*. 2013;72(2):278–285.
13. Nimmerjahn F, Bruhns P, Horiuchi K, Ravetch JV. FcγRIV: a novel FcR with distinct IgG subclass specificity. *Immunity*. 2005;23(1):41–51.
14. Nimmerjahn F, Ravetch JV. Fcγ receptors: old friends and new family members. *Immunity*. 2006;24(1):19–28.
15. Nimmerjahn F, Ravetch JV. Fc-receptors as regulators of immunity. *Adv Immunol*. 2007;96:179–204.
16. Nimmerjahn F, Ravetch JV. Fcγ receptors as regulators of immune responses. *Nat Rev Immunol*. 2008;8(1):34–47.
17. van Lent PL, et al. Fcγ receptors directly mediate cartilage, but not bone, destruction in murine antigen-induced arthritis: uncoupling of cartilage damage from bone erosion and joint inflammation. *Arthritis Rheum*. 2006;54(12):3868–3877.
18. van Lent PL, et al. Role of activatory FcγRI and FcγRIII and inhibitory FcγRII in inflammation and cartilage destruction during experimental antigen-induced arthritis. *Am J Pathol*. 2001;159(6):2309–2320.
19. van Vuuren AJ, et al. CD64-directed immunotoxin inhibits arthritis in a novel CD64 transgenic rat model. *J Immunol*. 2006;176(10):5833–5838.
20. Ellsworth JL, et al. Targeting immune complex-mediated hypersensitivity with recombinant soluble human FcγRIA (CD64A). *J Immunol*. 2008;180(1):580–589.
21. Ji H, et al. Arthritis critically dependent on innate immune system players. *Immunity*. 2002;16(2):157–168.
22. Brenn D, Richter F, Schaible HG. Sensitization of unmyelinated sensory fibers of the joint nerve to mechanical stimuli by interleukin-6 in the rat: an inflammatory mechanism of joint pain. *Arthritis Rheum*. 2007;56(1):351–359.
23. Ebbinghaus M, et al. The role of interleukin-1β in arthritic pain: main involvement in thermal, but not mechanical, hyperalgesia in rat antigen-induced arthritis. *Arthritis Rheum*. 2012;64(12):3897–3907.
24. Pinto LG, et al. IL-17 mediates articular hypernociception in antigen-induced arthritis in mice. *Pain*. 2010;148(2):247–256.
25. Richter F, et al. Interleukin-17 sensitizes joint nociceptors to mechanical stimuli and contributes to arthritic pain through neuronal interleukin-17 receptors in rodents. *Arthritis Rheum*. 2012;64(12):4125–4134.
26. Schaible HG. Nociceptive neurons detect cytokines in arthritis. *Arthritis Res Ther*. 2014;16(5):470.
27. Andoh T, Kuraishi Y. Direct action of immunoglobulin G on primary sensory neurons through Fcγ receptor I. *FASEB J*. 2004;18(1):182–184.
28. Qu L, Zhang P, LaMotte RH, Ma C. Neuronal Fc-γ receptor I mediated excitatory effects of IgG immune complex on rat dorsal root ganglion neu-

rons. *Brain Behav Immun*. 2011;25(7):1399–1407.
29. Qu L, Li Y, Pan X, Zhang P, LaMotte RH, Ma C. Transient receptor potential canonical 3 (TRPC3) is required for IgG immune complex-induced excitation of the rat dorsal root ganglion neurons. *J Neurosci*. 2012;32(28):9554–9562.
30. Miller RE, et al. Visualization of peripheral neuron sensitization in a surgical mouse model of osteoarthritis by in vivo calcium imaging. *Arthritis Rheumatol*. 2018;70(1):88–97.
31. van Lent PL, et al. Crucial role of synovial lining macrophages in the promotion of transforming growth factor β-mediated osteophyte formation. *Arthritis Rheum*. 2004;50(1):103–111.
32. Van Lent PL, Holthuysen AE, Van Rooijen N, Van De Putte LB, Van Den Berg WB. Local removal of phagocytic synovial lining cells by clodronate-liposomes decreases cartilage destruction during collagen type II arthritis. *Ann Rheum Dis*. 1998;57(7):408–413.
33. Qu L, Caterina MJ. Enhanced excitability and suppression of A-type K(+) currents in joint sensory neurons in a murine model of antigen-induced arthritis. *Sci Rep*. 2016;6:28899.
34. Verri WA, et al. IL-33 mediates antigen-induced cutaneous and articular hypernociception in mice. *Proc Natl Acad Sci U S A*. 2008;105(7):2723–2728.
35. Ioan-Facsinay A, et al. FcγRI (CD64) contributes substantially to severity of arthritis, hypersensitivity responses, and protection from bacterial infection. *Immunity*. 2002;16(3):391–402.
36. Ali EA, Barakat BM, Hassan R. Antioxidant and angiostatic effect of Spirulina platensis suspension in complete Freund's adjuvant-induced arthritis in rats. *PLoS One*. 2015;10(4):e0121523.
37. Fernandes ES, et al. A distinct role for transient receptor potential ankyrin 1, in addition to transient receptor potential vanilloid 1, in tumor necrosis factor α-induced inflammatory hyperalgesia and Freund's complete adjuvant-induced monarthritis. *Arthritis Rheum*. 2011;63(3):819–829.
38. Maiarù M, et al. The stress regulator FKBP51 drives chronic pain by modulating spinal glucocorticoid signaling. *Sci Transl Med*. 2016;8(325):325ra19.
39. Wahba MG, Messiha BA, Abo-Saif AA. Protective effects of fenofibrate and resveratrol in an aggressive model of rheumatoid arthritis in rats. *Pharm Biol*. 2016;54(9):1705–1715.
40. Moraes ER, Kushmerick C, Naves LA. Characteristics of dorsal root ganglia neurons sensitive to Substance P. *Mol Pain*. 2014;10:73.
41. Firestein GS. Immunologic mechanisms in the pathogenesis of rheumatoid arthritis. *J Clin Rheumatol*. 2005;11(3 suppl):S39–S44.
42. Boross P, et al. Destructive arthritis in the absence of both FcγRI and FcγRIII. *J Immunol*. 2008;180(7):5083–5091.
43. Díaz de Ståhl T, Andrén M, Martinsson P, Verbeek JS, Kleinau S. Expression of FcγRIII is required for development of collagen-induced arthritis. *Eur J Immunol*. 2002;32(10):2915–2922.
44. Magnusson SE, Engström M, Jacob U, Ulfgren AK, Kleinau S. High synovial expression of the inhibitory FcγRIIb in rheumatoid arthritis. *Arthritis Res Ther*. 2007;9(3):R51.
45. Matsui T, et al. CD64 on neutrophils is a sensitive and specific marker for detection of infection in patients with rheumatoid arthritis. *J Rheumatol*. 2006;33(12):2416–2424.
46. Matt P, Lindqvist U, Kleinau S. Elevated membrane and soluble CD64: a novel marker reflecting altered FcγR function and disease in early rheumatoid arthritis that can be regulated by anti-rheumatic treatment. *PLoS One*. 2015;10(9):e0137474.
47. Erbe DV, Collins JE, Shen L, Graziano RF, Fanger MW. The effect of cytokines on the expression and function of Fc receptors for IgG on human myeloid cells. *Mol Immunol*. 1990;27(1):57–67.
48. van der Poel CE, et al. Cytokine-induced immune complex binding to the high-affinity IgG receptor, FcγRI, in the presence of monomeric IgG. *Blood*. 2010;116(24):5327–5333.
49. Bullock CM, Wookey P, Bennett A, Mobasheri A, Dickerson I, Kelly S. Peripheral calcitonin gene-related peptide receptor activation and mechanical sensitization of the joint in rat models of osteoarthritis pain. *Arthritis Rheumatol*. 2014;66(8):2188–2200.
50. Ebbinghaus M, et al. Interleukin-6-dependent influence of nociceptive sensory neurons on antigen-induced arthritis. *Arthritis Res Ther*. 2015;17:334.
51. Liu XJ, et al. Nociceptive neurons regulate innate and adaptive immunity and neuropathic pain through MyD88 adapter. *Cell Res*. 2014;24(11):1374–1377.
52. Pohlers D, et al. Expression of cytokine mRNA and protein in joints and lymphoid organs during the course of rat antigen-induced arthritis. *Arthritis Res Ther*. 2005;7(3):R445–R457.
53. Bas DB, Su J, Wigerblad G, Svensson CI. Pain in rheumatoid arthritis: models and mechanisms. *Pain Manag*. 2016;6(3):265–284.
54. Paix A, et al. Precision genome editing using synthesis-dependent repair of Cas9-induced DNA breaks. *Proc Natl Acad Sci U S A*. 2017;114(50):E10745–E10754.
55. Xie T, et al. MicroRNA-127 inhibits lung inflammation by targeting IgG Fcγ receptor I. *J Immunol*. 2012;188(5):2437–2444.
56. Matousovic K, et al. IgA-containing immune complexes in the urine of IgA nephropathy patients. *Nephrol Dial Transplant*. 2006;21(9):2478–2484.
57. Jarvis JN, Taylor H, Iobidze M, Krenz M. Complement activation and immune complexes in children with polyarticular juvenile rheumatoid arthritis: a longitudinal study. *J Rheumatol*. 1994;21(6):1124–1127.
58. Dong P, Guo C, Huang S, Ma M, Liu Q, Luo W. TRPC3 is dispensable for β-alanine triggered acute itch. *Sci Rep*. 2017;7(1):13869.
59. Krenn V, et al. Synovitis score: discrimination between chronic low-grade and high-grade synovitis. *Histopathology*. 2006;49(4):358–364.
60. Pettit AR, et al. TRANCE/RANKL knockout mice are protected from bone erosion in a serum transfer model of arthritis. *Am J Pathol*. 2001;159(5):1689–1699.